The proton-activated receptor GPR4 modulates intestinal inflammation

Wang, Yu ; de Vallière, Cheryl ; Imenez Silva, Pedro H ; Leonardi, Irina ; Gruber, Sven ; Gerstgrasser, Alexandra ; Melhem, Hassan ; Weber, Achim ; Leucht, Katharina ; Wolfram, Lutz ; Hausmann, Martin ; Krieg, Carsten ; Thomasson, Koray ; Boyman, Onur ; Frey-Wagner, Isabelle ; Rogler, Gerhard ; Wagner, Carsten A

Abstract: BACKGROUND AND AIMS: During active inflammation tissue intraluminal intestinal pH is decreased in patients with inflammatory bowel disease (IBD). Acidic pH may play a role in IBD pathophysiology. Recently, proton sensing G-protein coupled receptors were identified, including GPR4, OGR1 (GPR68), and TDAG8 (GPR65). We investigated whether GPR4 is involved in intestinal inflammation. METHODS: The role of GPR4 was assessed in murine colitis models: chronic dextran sulphate sodium (DSS) administration and by crossbreeding into an IL-10 deficient background for development of spontaneous colitis. Colitis severity was assessed by body weight, colonoscopy, colon length, histological score, cytokine mRNA expression, and myeloperoxidase (MPO) activity. In the spontaneous Il-10-/- colitis model, the incidence of rectal prolapse and characteristics of lamina propria leukocytes (LPLs) were analyzed. RESULTS: Gpr4-/- mice showed reduced body weight loss and histology score after induction of chronic DSS colitis. In Gpr4-/- /Il-10-/- double knock-outs the onset and progression of rectal prolapse were significantly delayed and mitigated compared to Gpr4+/+ /Il-10-/- mice. Double knock-out mice showed lower histology scores, MPO activity, CD4 + T-helper cell infiltration, IFN- , iNOS, MCP-1 (CCL2), CXCL1 and CXCL2 expression compared to controls. In colon, GPR4 mRNA was detected in endothelial cells, some smooth muscle cells, and some macrophages. CONCLUSION: Absence of GPR4 ameliorates colitis in IBD animal models indicating an important regulatory rolein mucosal inflammation, thus providing a new link between tissue pH and the immune system. Therapeutic inhibition of GPR4 may be beneficial for the treatment of IBD.

DOI: https://doi.org/10.1093/ecco-jcc/jjx147

The proton-activated receptor

GPR4 modulates intestinal inflammation

Yu Wang[1,2*], Cheryl de Vallière[1*], Pedro H. Imenez Silva[2], Irina Leonardi[1], Sven Gruber[1,2], Alexandra Gerstgrasser[1], Hassan Melhem[1], Achim Weber[3], Katharina Leucht[1], Lutz Wolfram[1], Martin Hausmann[1], Carsten Krieg[4,5], Koray Thomasson[4], Onur Boyman[4,6], Isabelle Frey-Wagner[1], Gerhard Rogler[1,2§], Carsten A. Wagner[2§].

* Yu Wang and Cheryl de Valliere contributed equally to this work

§ Gerhard Rogler and Carsten A. Wagner share last authorship

[1] Department of Gastroenterology and Hepatology, University Hospital Zurich, Zurich, Switzerland.

[2] Institute of Physiology, University of Zurich, Zurich, Switzerland.

[3] Institute of Surgical Pathology, University Hospital Zurich, Zurich, Switzerland

[4] Laboratory of Applied Immunobiology, University of Zurich, Zurich, Switzerland.

[5] current address: Institute of Experimental Immunology, University of Zurich, Zurich, Switzerland.

[6] Department of Immunology, University Hospital Zurich, University of Zurich, Zurich, Switzerland.

SHORT TITLE: Gpr4 modulates colitis

Corresponding authors:

Prof. Dr. Carsten A. Wagner
University of Zurich
Institute of Physiology
Winterthurerstrasse 190
CH 8057 Zürich, Switzerland
Tel.: +41-44-5355023
Fax: +41-44-6356814
E-mail: Wagnerca@access.uzh.ch

Prof. Dr. Dr. Gerhard Rogler
Department of Gastroenterology and Hepatology
University Hospital Zurich
Rämistrasse 100
CH-8091 Zurich
Switzerland.
Tel.: +41 (0)44 255 95 19
Fax: +41 (0)44 255 94 97
Email: gerhard.rogler@usz.ch

Abstract

BACKGROUND AND AIMS: During active inflammation tissue intraluminal intestinal pH is decreased in patients with inflammatory bowel disease (IBD). Acidic pH may play a role in IBD pathophysiology. Recently, proton sensing G-protein coupled receptors were identified, including GPR4, OGR1 (GPR68), and TDAG8 (GPR65). We investigated whether GPR4 is involved in intestinal inflammation.

METHODS: The role of GPR4 was assessed in murine colitis models: chronic dextran sulphate sodium (DSS) administration and by crossbreeding into an IL-10 deficient background for development of spontaneous colitis. Colitis severity was assessed by body weight, colonoscopy, colon length, histological score, cytokine mRNA expression, and myeloperoxidase (MPO) activity. In the spontaneous *Il-10*$^{-/-}$ colitis model, the incidence of rectal prolapse and characteristics of lamina propria leukocytes (LPLs) were analyzed.

RESULTS: *Gpr4*$^{-/-}$ mice showed reduced body weight loss and histology score after induction of chronic DSS colitis. In *Gpr4*$^{-/-}$ */Il-10*$^{-/-}$ double knock-outs the onset and progression of rectal prolapse were significantly delayed and mitigated compared to *Gpr4*$^{+/+}$ */Il-10*$^{-/-}$ mice. Double knock-out mice showed lower histology scores, MPO activity, $CD4^+$ T-helper cell infiltration, IFN-γ, iNOS, MCP-1 (CCL2), CXCL1 and CXCL2 expression compared to controls. In colon, GPR4 mRNA was detected in endothelial cells, some smooth muscle cells, and some macrophages.

CONCLUSION: Absence of GPR4 ameliorates colitis in IBD animal models indicating an important regulatory rolein mucosal inflammation, thus providing a new link between tissue pH and the immune system. Therapeutic inhibition of GPR4 may be beneficial for the treatment of IBD.

Key Words: G-protein coupled receptor; pH receptors; GPR4; IBD; animal model.

Abbreviations: CCL20, chemokine (C-C motif) ligand 20; CD, Crohn's disease; CD31, cluster of differentiation 31; COX-2, prostaglandin-endoperoxide synthase 2; CXCL1, chemokine (C-X-C motif) ligand 1; CXCL2, chemokine (C-X-C motif) ligand 2; DSS, dextran sulphate sodium; GAPDH, glyceraldehyde-3-phosphate dehydrogenase; GPCR, G-protein coupled receptor; GPR4, G protein coupled receptor 4; H&E, hematoxylin and eosin; IBD, inflammatory bowel disease; ICAM-1, intercellular adhesion molecule 1; IFN-γ, interferon gamma; IL-10, interleukin 10; IL-18, interleukin 18; IL-6, interleukin 6; iNOS, nitric oxide synthase 2; LPLs, lamina propria leukocytes; MCP-1, chemokine (C-C motif) ligand 2, CCL2; MEICS, murine endoscopic index of colitis severity, MPO, myeloperoxidase; OGR1, ovarian cancer G protein coupled receptor 68 (also *Gpr68*); OR, odds ratio; PBS, phosphate buffered saline; RT-PCR, reverse transcription polymerase chain reaction; α-SMA, α-smooth muscle actin; SELE, selectin, endothelial cell; TDAG8, T-Cell Death-Activated Gene 8 (also known as G-protein coupled receptor *Gpr65*); TNF, tumor necrosis factor; UC, ulcerative colitis; VCAM1, vascular cell adhesion molecule 1.

Introduction

A local acidification in the gut lumen as well as in the mucosa has been observed during intestinal inflammation and implicated in the pathogenesis and progression of inflammatory bowel disease (IBD). Fallingborg *et al.* reported that intraluminal colonic pH values in the proximal parts of the colon were significnatly lower in patients with active ulcerative colitis (UC) than in normal subjects (lowest values 2.3, 2.9, and 3.4) [1]. Nugent and coworkers also reported a decrease of colonic luminal pH values to less than 5.5 in two out of six patients with active UC [2]. Also in patients with active Crohn's disease (CD) three out of four CD patients investigated had decreased pH values in the proximal colon (pH 5.3) and distal colon (pH 5.3) as compared to normal controls (pH 6.8) [2]. While there is still some controversy about the range of the intestinal luminal pH in IBD patients [3,4], it is widely accepted that inflammation is accompanied by tissue acidification due to hypoxia and excessive production and insufficient elimination of glycolytic metabolites. This indicates that luminal and tissue pH is decreased during active IBD. The (patho)physiological impact of these observations, however, has remained incompletely understood to date.

G protein-coupled receptors (GPCR) play an important role in regulating intestinal functions and have been implicated in the development and course of IBD [5-6]. Only recently, we found that the GPCR OGR1 (Ovarian cancer G-protein-coupled receptor 1, GPR68) plays a role in IBD and that genetic deletion of OGR1 partially prevents the development of colitis in the IL-10 deficient IBD mouse model [7]. The effects of OGR1 on intestinal function and inflammation may involve regulation of the intestinal barrier function [8.] OGR1 belongs to the same family of proton-activated G protein-coupled receptors as GPR4 [9-11]. A third family member is the T-cell death associated gene 8 (TDAG8, GPR65) [9-11]. Accumulating evidence indicates that members of this family of GPCRs, namely GPR4, OGR1 and TDAG8, are activated by protons upon a decrease of pH. At pH 7.6 the receptors are almost silent, while at pH 6.8 they

120 are fully activated and thus may play a crucial role in pH homeostasis [9,11].
121
122 GPR4 activation is transduced via the Ga_s pathway, followed by
123 intracellular cAMP accumulation [9,11]. Half-maximal activation of cAMP
124 formation by GPR4 expressed in HEK293 cells occurred at pH 7.55 [11]. Limited
125 studies exist on the relationship between GPR4 and tumor development or
126 regulation of metabolic acidosis in the kidney [12-18]. The function of all three
127 proton-activated receptors has been linked to inflammatory processes in
128 various tissues [19] but the role of GPR4 in IBD is currently unknown. *Gpr4*
129 mRNA was found to be widely expressed in a variety of tissues including small
130 intestine, colon, and spleen, and localized to - among other cell types -
131 endothelial cells throughout the body. In endothelial cells, activation of GPR4
132 by extracellular acidification stimulates proinflammatory pathways and
133 molecules involved in the adhesion of monocytes including CXCL2, CCL20,
134 VCAM1, and SELE [20]{Dong, 2013 #2467}{Tobo, 2015 #1}. Since GPR4 is
135 expressed along the small and large intestine, we hypothesized that this
136 proton-activated receptor might be involved in sensing local pH changes and
137 may participate in the pathophysiology of IBD.
138
139 Therefore, we examined the role of GPR4 in two murine models of colitis *in*
140 *vivo*, the dextran sulphate sodium (DSS) induced chronic colitis model and the
141 spontaneous colitis model in IL-10 deficient animals. Collectively, these data
142 demonstrate that absence of GPR4 is associated with ameliorated colitis,
143 indicating that pH sensing plays an important role in the pathophysiology of
144 IBD.
145
146
147
148
149
150
151
152

153 # Methods and Materials

154

155 ## Human colonic biopsies

156 Human colon biopsies were collected from patients during colonoscopy
157 performed at the Division of Gastroenterology and Hepatology, University
158 Hospital Zurich (Switzerland). CD patients (8 with severe, 7 with moderate
159 inflammation and 14 in remission) and UC patients (5 with severe and 3 with
160 moderate inflammation) underwent colonoscopy for assessment of
161 inflammation. Biopsies from patients with colitis were taken from inflamed
162 areas. The control biopsies (17 controls) were from subjects undergoing
163 colonoscopy for screening for colorectal cancer. The protocol for the study was
164 approved by the local Cantonal Ethics Committee Zurich, Switzerland.

165

166

167 ## *Induction of chronic colitis with DSS*

168 *Gpr4*$^{-/-}$ mice (BALB/c and C57BL/6 background) were provided by Thomas
169 Suply and Klaus Seuwen, Novartis, Basel [13,21]. *Gpr4*$^{-/-}$ mice (C57BL/6) were
170 bred to *Il10*$^{-/-}$ mice (C57BL/6) [22-24] with the goal to generate *Gpr4* $^{-/-}$ /*IL-10* $^{-/-}$
171 mice. All transgenic strains were bred in the standard animal facility of the
172 Institute of Physiology, University of Zurich. Animal experiments were
173 performed in the Zurich Integrative Rodent Physiology (ZIRP) core facility
174 according to the guidelines of the Swiss animal welfare law and approved by
175 the Cantonal Veterinary Office Zurich, Switzerland.

176 Three experiments (2 experiments on a BALB/c and one on a C57/BL6
177 background) were performed with DSS (MP Biomedicals, LLC, Solon, OH,
178 USA) induced chronic colitis. Female mice at the age of 10-13 weeks and a
179 body weight around 20 g were used in the experiment. Chronic colitis was
180 induced in wild-type and *Gpr4*$^{-/-}$ mice with 4 cycles of 3 % DSS in drinking
181 water for 7 days followed by 10 days of regular drinking water. After the last
182 cycle all animals were allowed to recover for 5 weeks and subsequently
183 sacrificed for sample collection. Mice on water served as controls throughout
184 the experiments.

In the spontaneous IL-10 deficient colitis model, the onset and development of inflammatory markers, colitis and rectal prolapses were monitored over 200 days and data was analyzed using Kaplan-Meier analysis (log rank Mantel-Cox test). For the evaluation by histology, flow cytometry, and for the determination of cytokine (mRNA) expression profiles, some mice were sacrificed by cervical dislocation at 80 days of age. For all experiments wild-type littermates were used.

Histological analysis was performed as described previously [25-27]. The sections were stained with hematoxylin and eosin (H&E) and scored by two independent researchers in a blinded fashion.

Data for the DSS colitis model originate from one round of experiments with mice with the identical genetic background (littermates) but the other two rounds of experiments yielded qualitatively similar results.

Genomic DNA extraction and genotyping

DNA extraction was done according to standard NaOH digestion. The PCR reactions used for GPR4 genotyping were set up with following oligonucleotides: 5'-atgggatcggccattgaacaa-3' (TS426), 5'-tcatcctgatcgacaagacc-3' (TS427), 5'- gctgccatgtggactctcga-3' (TS428), 5'-caggaaggcgatgctgatat-3' (TS429). TS426-TS427 is specific for neo (479 bps), and TS428-TS429 is specific for the GPR4 allele (302 bps). *IL-10* mice were screened with the following primers: forward 5'-GTGGGTGCAGTTATTGTCTTCCCG-3' (oIMR0086), reverse 5'-GCCTTCAGTATA AAA GGGGGACC-3'.

Assessment of colonoscopy score in mice

Mucosal damage was assessed by the murine endoscopic index of colitis severity (MEICS) as described previously [26-29]. Animals were anaesthetized intraperitoneally with 90-120 mg of ketamine (Narketan 10%, Vétoquinol AG, Bern, Switzerland) and 8 mg of xylazine (Rompun 2%, Bayer, Zurich,

Switzerland) per kg body weight and examined by colonoscopy (Karl Storz Tele Pack Pal 20043020, Karl Storz Endoskope, Tuttlingen, Germany).

Myeloperoxidase (MPO) activity assay

MPO activity was calculated by photoabsorbance, as previously described [26-27]. Briefly, colon tissues were homogenized in 50 mM phosphate buffered saline (PBS, pH 6.0) with 0.5% hexadecyltrimethylammonium bromide (H-5882, Sigma). After performing three cycles of freeze-and-thaw, 20 µl of the homogenates supernatant were mixed with 280 µl of 0.02% dianisidine (D-3252, Sigma) solution. After 20 min incubation at room temperature, absorbance was measured at 460 nm. Protein concentration of the colon tissue supernatant was determined by Bradford protein assay (Bio-Rad). MPO activity was calculated as mean absorbance/incubation time/protein concentration.

RNA extraction and quantitative Real-Time RT-PCR

Total RNA was extracted from colon and mesenteric lymph nodes tissue using the Qiagen RNeasy Mini Kit at a Qiacube workstation (Qiagen; Hilden, Germany) according to the manufacturer's instructions [26-27]. cDNA was prepared from adjusted RNA samples (2 µg/20 µl reaction) using the TaqMan High Capacity Reverse Transcriptase Reagent Kit (Applied Biosystems; Forster City, CA, USA). Thermocycling conditions for reverse transcription were set at 25 °C for 10 minutes, 37 °C for 120 minutes, 85 °C for 5 seconds (TGradient thermocycler, Biomera; Goettingen, Germany).

Semi-quantitative RT-PCR Taqman assays (7900 Fast Real Time PCR system, Applied Biosystems; Forster City, CA, USA) were performed under the following cycling conditions: 20 seconds at 95 °C, then 45 cycles of 95 °C for 3 seconds and 60 °C for 30 seconds with the TaqMan Fast Universal Mastermix. TaqMan assay probes for GPR4, TDAG8, OGR1, iNOS, IL-10, TNF-α, IFN-γ, IL-6, IL-18, MCP-1 (Life Technologies/ABI; Forster City, CA, USA) were used (Supplementary Table 1). RNA samples from individual animals were run in triplicates including a negative control (without cDNA). The comparative ΔCt method was applied to determine the quantity of the cytokines relative to the endogenous control *Gapdh* (mouse GAPDH, Mm03302249_g1, Reporter=VIC

and Quencher=MGB) and a reference sample. The relative quantification value was expressed and shown as $2^{-\Delta Ct}$.

RNA *in situ* hybridization (RNAscope) and immunohistochemistry

Il-10$^{-/-}$ (C57BL/6) and *Gpr4*$^{-/-}$ mice (C57BL/6) were used to examine where *Gpr4* mRNA is expressed in the murine proximal colon. C57BL/6 wild type mice were used as a wild-type reference (n=3 per strain). Proximal colon of isoflurane anesthetized mice was harvested and incubated for 24 hours in 4% paraformaldehyde/PBS. The PFA/PBS solution was replaced by 10% sucrose in PBS up to the tissue sink to the bottom of the container. This step was repeated with 20% and 30% sucrose solutions. Colon rings were cut and embedded in Optimal Cutting Temperature (OCT). Five µm sections were prepared on Superfrost microscope slides (Thermo Fisher Scientific, Braunschweig, Germany) and kept for up to one week at -80 °C. The RNA in situ hybridization was performed using the the RNAscope 2.5 HD assay, Red, and the RNAscope 2.0 HD detection kit, Brown (Advanced Cell Diagnostics, Hayward, CA, USA) following the manufacturer's protocol. Briefly, slides were rehydrated in PBS and were incubated with pretreatment solutions at recommended temperatures. Four signal amplification steps were performed at 40°C and two additional steps at room temperature with the appropriate solutions and probes designed and provided by the supplier (Advanced Cell Diagnostics, Hayward, CA, USA). The fifth amplification step was extended from 30 min to one hour in order to enhance the chromogenic signal. Detection of chromogenic signal was performed for 10 min using the specific reagents for the Red or Brown kit. RNA in situ hybridization with the RNAscope 2.5 HD assay, Red was followed by immunohistochemistry for cluster of differentiation 31 (CD31 or PECAM1), an endothelial marker, or immunofluorescence for α-Smooth Muscle Actin (α-SMA) or F4/80, a macrophage marker. Colon rings subjected to the combination of in situ hybridization for *Gpr4* with immunofluorescence for F4/80 and αSMA were incubated for 75 min at room temperature either with 1:10 rat anti-mouse F4/80 (MCA497R, Bio-Rad, Cressier, Switzerland) or with 1:50 rabbit anti-αSMA (Ab5694, Abcam, Cambridge, UK). Next slides were washed twice in hypertonic PBS (18g NaCl/l) and once in normal PBS, for 5 min each step. Secondary antibodies were

added to the sections for one hour at room temperature. Sections stained for F4/80 were combined with 1:500 goat anti-rat IgG (H+L) cross-absorbed secondary antibody, Alexa Fluor 488 (A11006, Thermo Fisher Scientific, Braunschweig, Germany) and sections stained for αSMA were combined with 1:500 donkey anti-rabbit IgG H&L, Alexa Fluor® 647 (ab150075, Abcam, Cambridge, UK). Slides were washed twice in hypertonic PBS and once in normal PBS, for 5 min each step and mounted with Dako glycergel mounting medium (Dako, Switzerland).

Colon rings subjected to the combination of in situ hybridization for *Gpr4* with immunohistochemistry for CD31, were incubated with Avidin/Biotin blocking reagents (Avidin/Biotin blocking kit, Vector Laboratories, Burlingame, CA, USA) and washed with PBS as described by the manufacturer. Next the tissue was incubated with 1:7 rat anti-mouse CD31 (550274, BD Pharmingen, USA) overnight at 4 °C, washed twice with PBS and incubated at room temperature for 30 min with 1:500 secondary antibody Biotin-SP-conjugated donkey anti-rat IgG (H+L) (Jackson ImmunoResearch, West Grove, PA, USA). The slides were washed twice in PBS and the immunohistochemical staining was obtained by incubating the colon sections for 30 min with Vecstatin Elite ABC reagent (Vector Laboratories, Burlingame, CA, USA). ABC solution was washed twice with PBS and replaced by DAB solution for 5 min (prepared as described by the manufacturer, Vector Laboratories, Burlingame, CA, USA). After washing for 5 min in water, slides were counterstained with hematoxylin I and the slides were mounted with VectaMount Mounting Medium HT-5000 (Vector Laboratories, Burlingame, CA, USA). Slides subjected to RNA in situ hybridization with RNAscope 2.0 HD detection kit, Brown were counterstained directly after the detection of the chromogenic signal.

Preparation of lamina propria lymphocytes (LPLs)

Lamina propria lymphocytes (LPLs) were isolated from *Gpr4*$^{-/-}$ /*Il-10*$^{-/-}$, *Gpr4*$^{+/+}$ /*Il-10*$^{-/-}$ and *Gpr4*$^{+/+}$ /*Il-10*$^{+/+}$ mice at 80 days of age following a modified protocol by Weigmann [30]. Briefly, the dissected colon was washed with Ca^{+}- and Mg^{+}-free PBS. The tissue was cut and incubated in medium containing 20 mM EDTA (Sigma-Aldrich) for 30 min at 37° C under shaking. LPLs were isolated from the lamina propria by enzymatic digestion (in DMEM

medium containing 300 U/mL collagenase type I, 2 mg/mL Hyaluronidase, 0.3 mg/ml DNase and 5 mM $CaCl_2.2H_2O$) for 15 min at 37 °C under shaking. The LPLs were purified by discontinuous Ficoll density-gradient centrifugation.

Flow Cytometric Analysis (FACS)

Single cell suspensions from lamina propria (LP) of mice were prepared as described above and stained for analysis by flow cytometry using PBS containing 4% fetal calf serum and 2.5 mM EDTA. At least 0.5×10^6 LP cells/well were stained at 4°C in the dark with the following fluorochrome-labeled monoclonal antibodies (all from BD Biosciences): α-CD3, α-CD4, α-CD8, α-CD25, α-CD45.2, and α-CD161 (NK1.1). Viable cells were acquired on a FACS Canto II (BD Biosciences) and analyzed using FlowJo software (TriStar Inc).

Statistical Analysis

Statistical analyses were performed using GraphPad Prism 5 (Version 5.04, GraphPad Software Inc, San Diego, CA, US) and SPSS (8.0 for Windows; SPSS Inc, Chicago, IL, US). Groups of data were compared between genotypes using nonparametric Mann-Whitney U-test or Kruskal-Wallis one-way ANOVA followed by Dunn's multiple-comparison test. All data were expressed as the means ± SEM. Probabilities (*p*, two tailed) of $p < 0.05$ were considered statistically significant. Body weight comparison was performed using "General Linear Model, repeated measures", and the full factorial model with type III sum of squares method [31]. The "General Linear Model, repeated measures" integrated both "individual deviation of daily body weight" and "difference in genotype groups" into the analysis to avoid systemic bias [31].

For prolapse rate comparison studies, statistical differences between genotypes were calculated by chi-square test with Fisher's exact test (exact significance, two sided) and risk estimate test from contingency table. The prolapse survival analysis was performed using Kaplan-Meier prolapse-free survival analysis (log-rank Mantel-Cox test) and estimated median prolapse-free survival time.

353

Results

IBD patients show enhanced GPR4 mRNA expression compared to healthy controls

According to the National Center for Biotechnology Information (NCBI) Gene Expression Omnibus (GEO) profile and Gene database (http://www.ncbi.nlm.nih.gov/sites/geo) [32] and the BioGPS database of The Scripps Research Institute (http://biogps.org)(e.g. GEO profile data set GDS3113 / 181558, GDS1096 / 211266_s_at, GDS1096 / 206236_at) [33], the human small intestine and colon express GRP4 at moderate levels (supplementary figure 1). GPR4 mRNA expression in the colon of healthy subjects and IBD patients was confirmed by RT-qPCR. GPR4 expression was significantly higher in UC (n=8) and CD (n=29) patients compared to healthy controls (n=17) (3.9 -fold, $P< 0.01$; 4.2 -fold, $P< 0.001$, respectively. Figure 1A). These results suggest that GPR4 may play a role during inflammation.

TDAG8 and OGR1 do not depend on GPR4 during DSS colitis in- mice

In wild-type mice, DSS-induced chronic colitis caused no upregulation of *Gpr4* mRNA expression in colonic tissue. While similar results for the two other members of the pH receptor family, TDAG8 and OGR1, were found upon adiminstration of DSS in both $Gpr4^{+/+}$ and $Gpr4^{-/-}$ mice (Figure 1B), which indicated that TDAG8 and OGR1 were not upregulated on mRNA level due to the lack of GPR4 *in vivo.*

Lack of GPR4 reduces inflammation in the chronic DSS model with ameliorated body weight recovery

Since GPR4 is expressed in human inflamed colonic tissue and proton-activated receptors have been linked to inflammatory diseases, we tested the impact of genetic deletion of GPR4 on the severity of chronic colitis in the DSS model. A total of 22 DSS treated $Gpr4^{+/+}$ (16 BALB and 6 C57BL/6) mice and 18 DSS treated $Gpr4^{-/-}$ (11 BALB and 7 C57BL/6) mice in 3 independent experiments were compared with 5 $Gpr4^{+/+}$ and 6 $Gpr4^{-/-}$ control mice (C57BL/6) receiving normal water. Compared with $Gpr4^{+/+}$ mice, $Gpr4^{-/-}$

mice showed less reduction in body weight upon DSS treatment (Fig. 2A). *Gpr4* $^{-/-}$ mice lost clearly less body weight (on Day 62: 2.7% vs *Gpr4*$^{+/+}$ + DSS mice: -1.5%) and from day 62 to day 83 showed an enhanced ability to regain weight ($P< 0.05$ *, Figure 2A). All 3 independent experiments showed similar results: *Gpr4* $^{-/-}$ mice recovered with higher body weights indicating that GPR4 deficiency ameliorated inflammation-associated body weight changes ($P< 0.05$ for BALB (exp 1 and 2) and $P< 0.01$ ** for C57BL/6).

Colonic specimens from all groups were analyzed for severity of inflammation by histological scoring by two blinded experts as described previously [8]. The histological score was significantly lower in *Gpr4* $^{-/-}$ mice with DSS induced chronic colitis (Figure 2B,C and supplementary figure 2) compared to wild-type controls (2.3 ± 0.38 vs. 4.9 ± 0.81; $P< 0.001$) (supplementary figure 1A). DSS treated *Gpr4*$^{-/-}$ mice had lower scores for both epithelial injury and leukocyte infiltration ($P< 0.001$ each) (Figure 2B and 2C). All 3 experiments showed consistent results independent of genetic background. In contrast, DSS treated *Gpr4*$^{-/-}$ had slightly shorter colon lengths and a higher endoscopic MEICS score ($P< 0.05$, Supplementary Figure 3A and 3B). GPR4 deficiency did not influence MPO activity and spleen weight upon colitis induction (Supplementary Figure 3C and 3D). No differences in the cytokine expression profiles of iNOS, IL-10, TNF-α, IL-6, and MCP-1 from colon and mesenteric lymph nodes of DSS induced colitis *Gpr4*$^{+/+}$ and *Gpr4*$^{-/-}$ mice were observed (Figure 3 and Supplementary Figure 3E). Only IFN-γ mRNA expression in colon samples was higher in *Gpr4*$^{-/-}$ mice treated with DSS compared to in wild-type mice receiving DSS (Figure 3).

Spontaneous colitis in the IL-10 KO mouse is attenuated by GPR4 deficiency

The impact of GPR4 in colitis development was further assessed in the spontaneous colitis model in IL10 deficient animals. All mice were maintained in the same animal housing room and all experiments were carried out during the same time period. The occurrence of rectal prolapse as a sign of spontaneous colitis in *Il-10*$^{-/-}$ mice was monitored for 200 days. No prolapses

were observed in control *Gpr4*$^{+/+}$ /*Il-10*$^{+/+}$ mice in the breeding colonies for 200 days (n > 100 for each gender). In comparison with *Gpr4*$^{+/+}$ /*Il-10*$^{-/-}$ mice, both female and male *Gpr4*$^{-/-}$ /*Il-10*$^{-/-}$ mice, had a significantly lower rectal prolapse incidence (female: 6.9%, n = 29 vs. 66.7%, n = 12, *P*< 0.001, odds ratios of *Gpr4*$^{-/-}$/*Gpr4*$^{+/+}$ = 0.037 (95% CL 0.006-0.241); male: 24.4%, n=41 vs. 52.0%, n=25, *P*= 0.033, odds ratios = 0.298 (95% CL 0.103-0.859); chi-square test with Fisher's exact test/two sided).

Kaplan-Meier prolapse-free survival analysis showed a significantly delayed onset of rectal prolapse in *Gpr4*$^{-/-}$ /*Il-10*$^{-/-}$ mice as compared to *Gpr4*$^{+/+}$ /*Il-10*$^{-/-}$ mice (estimated median prolapse-free survival time, female: >200 days vs. 123 days, *P*< 0.001; male: >200 days vs. 161 days, *P*= 0.007, log rank (Mantel-Cox) test, Figure 4A and Supplementary Figure 5A).

Figure 4B (and Supplementary Figure 5B) illustrate the level of granulocyte infiltration as measured by MPO activity in colon tissue of mice at 80 days of age. This age was chosen as none of the mice had developed a prolapse at this age. In *Gpr4*$^{-/-}$ /*Il-10*$^{-/-}$ male mice, MPO activity was significantly lower than that in *Gpr4*$^{+/+}$ /*Il-10*$^{-/-}$ male mice (0.013 ± 0.068 vs. 0.53 ± 0.101, *P*< .05). A similar trend was seen in female *Gpr4*$^{-/-}$ /*Il-10*$^{-/-}$ animals (Figure 4B).

Histological scoring by two blinded investigators of 80 days old mice showed that colons from male (histological score of 1.6 ± 0.91) and female (1.6 ± 0.93) *Gpr4*$^{+/+}$ /*Il-10*$^{+/+}$ mice were morphologically normal. *Gpr4*$^{-/-}$ /*Il-10*$^{-/-}$ male (2.3 ± 0.68) and female (2.6 ± 1.69) mice displayed significantly less mucosal injury and infiltration as compared to *Gpr4*$^{+/+}$ /*Il-10*$^{-/-}$ male (6.3 ± 0.45) and female (6.5 ± 1.12) mice (*P*< 0.05 for both) (Figure 5A and B and Supplementary Figures 4 and 6), consistent with the prolapse ratio and prolapse-free survival analysis.

Reduction of mucosal CD4+ T helper cell infiltrate upon *Gpr4* deficiency

Spontaneous colitis in IL-10 deficient mice is mediated by Th1 and Th17 cell infiltration [34-35]. In order to identify cellular players underlying the reduced colitis in *Gpr4*$^{-/-}$ mice we subsequently analyzed cellular infiltrates in the lamina propria by flow cytometry. As shown in Figure 6 and Supplementary Figure 6,

the percentage of total CD4+ cells and the CD4+ to CD8+ ratios in the lamina propria were significantly higher in *Gpr4*$^{+/+}$ /*Il-10*$^{-/-}$ as compared to wild-type controls ($P < .01$, $P < 0.001$ and $P < 0.001$). *Gpr4*$^{+/+}$ /*Il-10*$^{-/-}$ mice had significantly higher counts of CD4+ cells, but not of CD8+ cells in the lamina propria. The percentage of CD4+ of CD3+ was significantly lower in *Gpr4*$^{-/-}$ /*Il10* $^{-/-}$ ($P < 0.05$, Figure 6) whereas no differences of regulatory T cells, natural killer cells, total CD45+ cells, monocytes/macrophages and neutrophils in LPLs composition were observed among the three groups (Supplementary Table 2).

GPR4 modulates expression of factors involved in inflammation

We further characterized mRNA expression of cytokines and other factors involved in cell adhesion and shown to be regulated by GPR4[36] in colon tissue and mesenteric lymph nodes using age-matched female (Figure 7 and Supplementary Figure 8) and male (Supplementary Figure 9) mice at 80 days of age. As shown in Figure 7**,** iNOS, IFN-γ, MCP-1, CXCL1, and CXCL2 mRNA expression was significantly lower in the colon of *Gpr4*$^{-/-}$ /*Il-10*$^{-/-}$ mice ($P < .05$), which reconfirmed reduced Th1-cell infiltrates in mice lacking GPR4. Furthermore, *Gpr4*$^{-/-}$ /*Il-10*$^{-/-}$ mice showed a trend for lower mRNA expression of IL-6, SELE, VCAM1 as compared to *Gpr4*$^{+/+}$ /*Il-10*$^{-/-}$ mice (Figure 7 and Supplementary Figure 8). Male mice had similar patterns of changes in colon (Supplementary Figures 9). However, in lymph nodes from female and male mice no clear differences could be detected (Supplementary Figures 8B).

Localization of *Gpr4* mRNA in colon tissue

Lastly, we performed chromogenic RNA *in situ* hybridization of Gpr4 mRNA (RNAscope) in the proximal colon to examine where GPR4 may act to modulate inflammation. The tissue viability and assay quality were tested with the positive control Peptidyl-prolyl cis-trans isomerase B **(***Ppib***)** and a probe for the bacterial gene dihydrodipicolinatereductase **(***Dapb***)** (data not shown) was used as an additional negative control to *Gpr4*$^{-/-}$. Wild-type and *Il10*$^{-/-}$ mice displayed chromogenic signals in lamina propria and muscularis (Figure 8 and Supplementary Figure 10), whilst the signal was absent from Gpr4$^{-/-}$ colon (supplementary Figure 11). Gpr4 mRNA related signal was prominent in cells lining small vessels consistent with the localization of Gpr4 in endothelial cells.

Signal intensity appeared to be higher in colon from *Il10*$^{-/-}$ mice and was also found in cells clustering in the interstitium. Costaining with CD31, a marker of endothelial cells, demonstrated partial colocalization of the Gpr4 signal with CD31. However, cells in the muscularis as well as clusters of interstitial cells, particularly abundant in colon from *Il10*$^{-/-}$ mice, were positive for Gpr4 and negative for CD31. (Figure 8). Further colocalization studies demonstrated partial colocalization of Gpr4 mRNA with α-smooth muscle actin, particularly seen in the muscularis layer (Figure 9A-D). Moreover, costainings with F4/80, a marker for macrophages, detected some macrophages with positive staining for Gpr4 mRNA (Figure 9E-H) both in the colon of WT and *Il10*$^{-/-}$ mice.

Discussion

This is the first detailed study on the (patho-)physiological function of the proton-activated G-protein coupled receptor GPR4 in the intestine and its impact on chronic intestinal inflammation. We demonstrate that GPR4 deletion protects against experimental colitis in both DSS-induced chronic colitis and the spontaneous colitis observed in IL-10 deficient mice.

We show that GPR4 mRNA is expressed in the muscularis and lamina propria of colon and is strongly up-regulated in the colons of IBD patients. The localization based on mRNA in-situ hybridization is consistent with reports suggesting a predominant expression of GPR4 in endothelial cells [37]. However, also smooth muscle cells in the muscularis and some macrophages showed expression of Gpr4. In the chronic DSS colitis model [34-35,38-39], *Gpr4*$^{-/-}$ mice lost less body weight and had lower histology scores compared to wild-type littermates indicating less severe inflammation. In the spontaneous IL-10 deficient colitis model [22-24] lack of GPR4 significantly delayed onset and progression of rectal prolapses. As IL-10 is a well-known anti-inflammatory cytokine and suppressive for Th1 cells and macrophages [40], IL-10 knockout mice are thought to have a Th1-cell driven disease [34-35]. Consistent with reduced Th1 cell infiltrates in *Gpr4* $^{-/-}$ */IL-10* $^{-/-}$ mice, a significantly lower IFN-γ expression was found. Also, iNOS, MCP-1, CXCL1, and CXCL2 were reduced in the absence of GPR4. Further, flow cytometry analysis demonstrated that GPR4 knockout mice exhibit reduced infiltration of CD4+ T cells into the colon. The anti-inflammatory effect of GPR4 deficiency seemed not to be mediated by a regulatory T cell dependent mechanism as no significant differences in regulatory T cell numbers were observed between groups. However, we cannot exclude a functional change of regulatory T cells in GPR4-deficient animals.

Therefore, activation of GPR4 is likely to exacerbate intestinal inflammation. Based on the expression of GPR4 in endothelial cells, the fact that GPR4 in a pH-dependent fashion triggers expression of pathways involved in cell adhesion and inflammation in endothelial cells, and that

endothelial cells can recruit and regulate inflammatory cells, we hypothesize that GPR4 may play a role in modulating inflammation in IBD. The down-stream signals may involve, among others, the IFN-γ pathway. IFN-γ aggravates inflammation by increasing iNOS expression, activating macrophages and natural killer cells, favoring Th1 cell immune responses, and inducing apoptosis [41-42]. Also, Gpr4 positive macrophages may contribute to inflammation. The role of Gpr4 in smooth muscle cells, however, remains elusive at this point. The excessive production of glycolytic metabolites in inflamed tissue causes the accumulation of protons, which may further activate GPR4, contributing to a positive feedback loop which may lead to a vicious cycle. Thus blockade of GPR4 may be a promising new target for IBD treatment.

In vitro stimulation of GPR4 caused upregulation of many transcripts involved in inflammatory processes [36]. Recent data published on *Gpr4* $^{-/-}$ mice support the deleterious role of GPR4 activation during inflammation. Reduced immune responses and attenuated airway hyper-responsiveness were observed in GPR4 deficient mice following ovalbumin exposure [43]. This was accompanied by a reduction in the number of eosinophils in broncho-alveolar lavage fluid [44]. In the cigarette smoke-induced COPD mouse model, *Gpr4* $^{-/-}$ mice had accelerated elimination of airway inflammation and enhanced neutrophil clearance [45]. In patients with systemic sclerosis, expression of GPR4 correlates with the severity of lung disease [46]. Similarly, a study published during the preparation of this manuscript describes a role of GPR4 in aggravating the response to an acute DSS-mediated colonic chemical insult [37].

Yang *et al*. found evidence that acidosis/GPR4 signaling regulates endothelial cell adhesion mainly through the Gs/cAMP/Epac pathway [20]. The activation of GPR4 by acidosis up-regulated the expression of multiple adhesion molecules such as SELE, VCAM-1 and ICAM-1 in vitro and increased the adhesiveness of human umbilical vein endothelial cells (HUVECs) expressing endogenous GPR4. These adhesion molecules are involved in the binding of leukocytes [20]. In our studies *Gpr4*$^{-/-}$ */Il-10*$^{-/-}$ mice

expressed lower mRNA levels of iNOS, TNF-α, IFN-γ, IL-6, MCP-1, CXCL2, CXCL1, SELE and VCAM-1 which at least in part is in agreement with the mentioned *in vitro* observations. A regulation of the NF-κB pathway by GPR4-dependent signaling has been postulated [36] further supporting our findings.

In summary, our results demonstrate that GPR4^{-} deficiency protects from experimental colitis in two different mouse models indicating an important pathophysiological role for the proton-activated receptor during the pathogenesis of mucosal inflammation. Future research needs to address the role of GPR4 in human IBD. Based on our mouse data, GPR4 may become a promising novel target for pharmacological IBD therapy.

Acknowledgement

We thank Prof. Dr. Burkhardt Seifert and Dr. Sarah R. Haile (Division of Biostatistics, University of Zurich) for the statistics support and advice. We also thank Dr. Klaus Seuwen, Novartis Institutes for BioMedical Research (NIBR), Basel, Switzerland, for his critical comments and valuable suggestions as well as for providing the *Gpr4* KO mice. Parts of the study were presented at the Digestive Disease Week (DDW) 2011 (Chicago, IL) and DDW 2012 (San Diego, CA), and the Annual Meeting of the Swiss Physiological Society and Young Investigator Award 2012 (Fribourg, Switzerland).

This work was supported by a collaborative grant for the Zurich Center for Integrative Human Physiology (ZIHP) to A. Weber, O. Boyman, G. Rogler, and C.A. Wagner, and by grants from the Swiss National Science Foundation to C.A. Wagner (31003A_155959/1) and G. Rogler (153380 and 148422). P. H. Imenez Silva has been a recipient of a fellowship from the IKPP Kidney.CH under the European Unions Seventh Framework Programme for Research, Technological Development and Demonstration under the grant agreement no 608847 and Conselho Nacional de Desenvolvimento Científico e Tecnológico (CNPq) grant number 205625/2014-2.

Authors contribution

YWang, CdeValliere, ILeonardi, PHISilva, SGruber, AGerstgrasser, HMelham, KLeucht, LWolfram, MHausmann, CKrieg, KThomasson performed experiments; YWang, CdeValliere, ILeonardi, SGruber, AGerstgrasser, AWeber, KLeucht, LWolfram, MHausmann, CKrieg, OBoyman, IFrey-Wagner, GRogler, CAWagner analyzed data; OBoyman, IFrey-Wagner, GRogler, CAWagner planned experiments; OBoyman, GRogler, CAWagner obtained funding for the project; YWang, GRogler, CAWagner wrote the manuscript; all authors read and approved the manuscript.

Conflict of interests

All authors declare that they have no conflict of interests that influenced design, performance, analysis and interpretation of experiments.

Figure legends

Figure 1

GPR4 mRNA detection in colonic tissue from humans and mice.

(A) *GPR4* mRNA was detected in colonic biopsies from controls (normal subjects), and patients with ulcerative colitis (UC), or Crohn's disease (CD) by real-time RT-PCR Taqman assays. A minimum of 5 patients per group was tested for quantification. **(B)** *Gpr4, Tdag8 and Ogr1* mRNA detection in colonic tissues from wild-type mice or *Gpr4* $^{-/-}$ mice with water or DSS induced chronic colitis. Groups of data were compared between control group and different individual group using the non-parametric Kruskal-Wallis one-way ANOVA followed by Dunn's multiple-comparison test. For quantification, values are mean ± SEM; n ≥ 5 per group; P<0.01 **, P < 0.001 ***.

Figure 2

***Body* weight loss analysis and histological assessment of colonic inflammation.**

(A) *Gpr4* $^{-/-}$ mice, compared with *Gpr4* $^{+/+}$ mice, showed less relative body weight loss during DSS-induced chronic colitis. After 4 cycles of DSS treatment (last 22 days), *Gpr4* $^{-/-}$ mice exhibited clearly reduced gain of body weight (F=2.980, P< .05 *) than *Gpr4* $^{+/+}$ mice. The body weight changes are expressed as relative change of body weight in % relative to day 0. Histology scores were analyzed to assess the epithelial damage **(B)** and leukocyte infiltration **(C)** indicating less severe inflammation in *Gpr4* $^{-/-}$ mice with DSS. The right panel shows a representative histological section from wild-type or *Gpr4* $^{-/-}$ mice treated with DSS, scale bar 100 μm. Data are representative of 3 independent experiments each with 6-8 female mice/ group.

Figure 3

Assessment of the colitis severity during DSS induced chronic colitis. The mRNA expression levels of iNOS, IL-10, TNF-α, IFN-γ, IL-6, and MCP-1 in

colon from *Gpr4* $^{-/-}$ mice and *Gpr4* $^{+/+}$ mice with or without administration of DSS were not changed between genotypes for the same treatment. For quantification, values are mean ± SEM; n ≥ 5 per group; $P < 0.05$ *, $P < 0.01$ **, $P < 0.001$ ***. Data are representative of 3 independent experiments.

Figure 4

Development of IBD and progression to prolapse were reduced by the deletion of GPR4 from IL10 deficient mice.

(A) Kaplan-Meier prolapse-free survival curve showed delayed onset and progression of prolapses in female *Gpr4*$^{-/-}$ /*Il-10*$^{-/-}$ mice relative to female *Gpr4*$^{+/+}$ /*Il-10*$^{-/-}$ mice (estimated median prolapse-free survival time, >200 days vs. 123 days, $P< 0.001$ ***, log rank (Mantel-Cox) test). Black dotted lines, *Gpr4*$^{-/-}$ /*Il-10* $^{-/-}$ mice (6.9% prolapses, n=29, female); black solid line, *Gpr4* $^{+/+}$ /*Il-10*$^{-/-}$ mice (66.7% prolapses, n=12, female); grey dotted lines, *Gpr4*$^{+/+}$ /*Il-10*$^{+/+}$ mice (0% prolapses, n=31, female). No rectal prolapse was detected in the *Gpr4*$^{+/+}$ /*Il-10*$^{+/+}$ mice in these breeding colonies for 200 days (> 100 mice). Comparison of MPO activity in colon tissue **(B)**, colon length **(C),** and relative spleen weight **(D)** showed attenuated colitis in female *Gpr4*$^{-/-}$ /*Il-10*$^{-/-}$ mice (not significant but relative spleen weight, $P< 0.01$ **, Kruskal-Wallis one-way ANOVA followed by Dunn's multiple-comparison test).

Figure 5

Less histological damage in *Gpr4*$^{-/-}$ /*Il-10*$^{-/-}$ female mice.

(A) The total histology scores of distal colon of female *Gpr4*$^{-/-}$ /*Il-10*$^{-/-}$, *Gpr4*$^{+/+}$ /*Il-10*$^{-/-}$ and *Gpr4*$^{+/+}$ /*Il-10*$^{+/+}$ mice at 80 days of age are shown, indicating reduced inflammation in *Gpr4*$^{-/-}$ /*Il-10*$^{-/-}$ mice ($P< 0.05$, *Gpr4*$^{-/-}$ /*Il-10*$^{-/-}$ compared to *Gpr4*$^{+/+}$ /*Il-10*$^{-/-}$*)*. **(B)** H&E stained sections showed the significant difference in the damage of epithelial integrity and intensity of the leukocyte infiltration into inflamed sites. Scale bar 100 μm. The total histology scores are representative for overall histology scores of distal colon (epithelial injury plus leukocyte infiltration). Data are presented as mean ± SEM; n ≥ 5 per group; $P < 0.05$ *, $P <0 .01$ **, $P < 0.001$ ***.

Figure 6

Suppression of IFN-γ-producing CD4$^+$ T helper cells in *Gpr4$^{-/-}$* /*Il-10$^{-/-}$* mice.

LPLs were isolated from the colon of female *Gpr4$^{-/-}$* /*Il-10$^{-/-}$*, *Gpr4$^{+/+}$* /*Il-10$^{-/-}$* and *Gpr4$^{+/+}$* /*Il-10$^{+/+}$* mice, stained to identify subpopulations and analyzed by flow cytometry. LPL profiles from flow cytometry analysis demonstrated that ablation of GPR4 suppressed accumulation of CD4$^+$ (T helper) cells, mainly Th1 cells, but not CD8$^+$ (T cytotoxic) cells: quantification of CD4$^+$ T cells, percentage of CD4$^+$ within CD3$^+$ T cells, CD4$^+$/CD8$^+$ ratio, quantification of CD8$^+$ T cells, and percentage of CD8$^+$ within CD3$^+$ T cells. The difference between *Gpr4$^{-/-}$* /*Il-10$^{-/-}$* and *Gpr4$^{+/+}$* /*Il-10$^{-/-}$* did not reach statistical significance. Representative flow cytometry data of more than 5 qualitatively similar experiments are shown; isolated LPLs from 3 female mice were pooled in each group. Data are presented as mean ± SEM; $P < 0.05$ *, $P < 0.01$ **, $P < 0.001$ ***.

Figure 7

Analysis of mRNA expression profiles of cytokines in colon from *Gpr4$^{-/-}$* /*Il-10$^{-/-}$*, *Gpr4$^{+/+}$* /*Il-10$^{-/-}$* and *Gpr4$^{+/+}$* /*Il-10$^{+/+}$* mice.

The mRNA expression profiles of iNOS, IFN-γ, IL-6, MCP-1, CXCL1, and CXCL1 were analyzed by semi-quantitative RT-qPCR in colon tissue from of all three female strains (*Gpr4$^{-/-}$* /*Il-10$^{-/-}$*, *Gpr4$^{+/+}$* /*I-10$^{-/-}$* and *Gpr4$^{+/+}$* /*Il-10$^{+/+}$* mice). Th1 associated IFN-γ expression was significantly lower in colon of female *Gpr4$^{-/-}$* /*IL-10$^{-/-}$* mice compared with female *Gpr4$^{+/+}$* /*Il-10$^{-/-}$* mice ($P < 0.05$ *, Kruskal-Wallis one-way ANOVA followed by Dunn's multiple-comparison test). Data are presented as relative expression normalized to the house-keeping gene GAPDH, n = 6-9 mice per group. Data are presented as mean ± SEM; *P*

711 < 0.05 *, *P* < 0.01 **, *P*< 0.001 ***.
712
713
714 ***Figure 8***
715 **Localization of Gpr4 mRNA in endothelial cells in the colon from *Gpr4*$^{+/+}$**
716 **and *Il10*$^{-/-}$ mice.**
717 Chromogenic in-situ hybridization of Gpr4 mRNA (red dots) in murine proximal
718 colon using RNAscope. Sections were also labeled with antibodies against
719 CD31, a marker of endothelial cells, showing partial colocalization with Gpr4.
720 **(A-C)** Wild-type colon, **(D-F)** Colon from *Il10*$^{-/-}$. Arrows indicate representative
721 areas with Gpr4 mRNA expression. Scale bar 50 μm. Inserts show higher
722 magnifications.
723
724 ***Figure 9***
725 **Localization of Gpr4 mRNA in smooth muscle cells and macrophages in**
726 **the colon from *Gpr4*$^{+/+}$ and *Il10*$^{-/-}$ mice.**
727 Fluorescent in-situ hybridization of Gpr4 mRNA (red dots) in murine proximal
728 colon using RNAscope. **(A-D)** Sections were also labeled with antibodies
729 against α-smooth muscle actin (green), a marker of smooth muscle cells
730 showing partial colocalization with Gpr4. **(E-H)** Costaining for F4/80 (green), a
731 marker for macrophages, detected staining of some macrophages, see insert.
732 Nuclei were stained with DAPI (blue). Scale bar 50 μm. Inserts show higher
733 magnifications.
734
735
736

References

1. Fallingborg J, Christensen LA, Jacobsen BA, Rasmussen SN. Very low intraluminal colonic pH in patients with active ulcerative colitis. *Dig Dis Sci* 1993;**38**:1989-93.

2. Nugent SG, Kumar D, Rampton DS, Evans DF. Intestinal luminal pH in inflammatory bowel disease: Possible determinants and implications for therapy with aminosalicylates and other drugs. *Gut* 2001;**48**:571-7.

3. Press AG, Hauptmann IA, Hauptmann L*, et al.* Gastrointestinal pH profiles in patients with inflammatory bowel disease. *Aliment Pharmacol Ther* 1998;**12**:673-8.

4. Ewe K, Schwartz S, Petersen S, Press AG. Inflammation does not decrease intraluminal pH in chronic inflammatory bowel disease. *Dig Dis Sci* 1999;**44**:1434-9.

5. Lee T, Lee E, Arrollo D, Lucas PC, Parameswaran N. Non-hematopoietic beta-arrestin1 confers protection against experimental colitis. *J Cell Physiol* 2016;**231**:992-1000.

6. Li X, Murray F, Koide N*, et al.* Divergent requirement for Galphas and cAMP in the differentiation and inflammatory profile of distinct mouse Th subsets. *J Clin Invest* 2012;**122**:963-73.

7. de Valliere C, Wang Y, Eloranta JJ*, et al.* G protein-coupled pH-sensing receptor OGR1 is a regulator of intestinal inflammation. *Inflamm Bowel Dis* 2015;**21**:1269-81.

8. de Valliere C, Vidal S, Clay I*, et al.* The pH-sensing receptor OGR1 improves barrier function of epithelial cells and inhibits migration in an acidic environment. *Am J Physiol Gastrointest Liver Physiol* 2015;**309**:G475-90.

9. Seuwen K, Ludwig MG, Wolf RM. Receptors for protons or lipid messengers or both? *J Recept Signal Transduct Res* 2006;**26**:599-610.

10. Choi JW, Lee SY, Choi Y. Identification of a putative G protein-coupled receptor induced during activation-induced apoptosis of T cells. *Cell Immunol* 1996;**168**:78-84.

11. Ludwig MG, Vanek M, Guerini D*, et al.* Proton-sensing G-protein-coupled receptors. *Nature* 2003;**425**:93-8.

12. Sin WC, Zhang Y, Zhong W*, et al.* G protein-coupled receptors GPR4 and TDAG8 are oncogenic and overexpressed in human cancers. *Oncogene* 2004;**23**:6299-303.

13. Wyder L, Suply T, Ricoux B*, et al.* Reduced pathological angiogenesis and tumor growth in mice lacking GPR4, a proton sensing receptor. *Angiogenesis* 2011;**14**:533-44.

14. Sun X, Yang LV, Tiegs BC*, et al.* Deletion of the pH sensor GPR4 decreases renal acid excretion. *J Am Soc Nephrol* 2010;**21**:1745-55.

15. Codina J, Opyd TS, Powell ZB*, et al.* pH-dependent regulation of the alpha-subunit of H+-K+-ATPase (HKalpha2). *Am J Physiol Renal Physiol* 2011;**301**:F536-43.

16. Castellone RD, Leffler NR, Dong L, Yang LV. Inhibition of tumor cell migration and metastasis by the proton-sensing GPR4 receptor. *Cancer Lett* 2011;**312**:197-208.

17. Brown D, Wagner CA. Molecular mechanisms of acid-base sensing by the kidney. *J Am Soc Nephrol* 2012;**23**:774-80.

18. Wagner CA. Metabolic acidosis: New insights from mouse models. *Curr Opin Nephrol Hypertens* 2007;**16**:471-6.

19. Okajima F. Regulation of inflammation by extracellular acidification and proton-sensing GPCRs. *Cell Signal* 2013;**25**:2263-71.

20. Chen A, Dong L, Leffler NR*, et al.* Activation of GPR4 by acidosis increases endothelial cell adhesion through the cAMP/EPAC pathway. *PLoS One* 2011;**6**:e27586.

21. Kumar NN, Velic A, Soliz J*, et al.* Physiology. Regulation of breathing by CO_2 requires the proton-activated receptor GPR4 in retrotrapezoid nucleus neurons. *Science* 2015;**348**:1255-60.

22. MacDonald TT. Gastrointestinal inflammation. Inflammatory bowel disease in knockout mice. *Curr Biol* 1994;**4**:261-3.

23. Bhan AK, Mizoguchi E, Smith RN, Mizoguchi A. Colitis in transgenic and knockout animals as models of human inflammatory bowel disease. *Immunol Rev* 1999;**169**:195-207.

24. Michelle E.A. Borm, Bouma. G. Animal models of inflammatory bowel disease. *Drug discovery today: Disease models*: Elsevier; 2004: 437-43.

25. Hausmann M, Obermeier F, Paper DH*, et al.* In vivo treatment with the herbal phenylethanoid acteoside ameliorates intestinal inflammation in dextran sulphate sodium-induced colitis. *Clin Exp Immunol* 2007;**148**:373-81.

26. Bentz S, Pesch T, Wolfram L*, et al.* Lack of transketolase-like (tktl) 1 aggravates murine experimental colitis. *Am J Physiol Gastrointest Liver Physiol* 2011;**300**:G598-607.

27. Fischbeck A, Leucht K, Frey-Wagner I*, et al.* Sphingomyelin induces cathepsin d-mediated apoptosis in intestinal epithelial cells and increases inflammation in dss colitis. *Gut* 2011;**60**:55-65.

28. Becker C, Fantini MC, Neurath MF. High resolution colonoscopy in live mice. *Nat Protoc* 2006;**1**:2900-4.

29. Scharl M, Leucht K, Frey-Wagner I*, et al.* Knock-out of beta-glucosidase 2 has no influence on dextran sulfate sodium-induced colitis. *Digestion* 2011;**84**:156-67.

30. Weigmann B, Tubbe I, Seidel D*, et al.* Isolation and subsequent analysis of murine lamina propria mononuclear cells from colonic tissue. *Nat Protoc* 2007;**2**:2307-11.

31. SPSS Inc. *SPSS advanced statistics 17.0*. Chicago, Ill.: SPSS Inc.; 2007.

32. NCBI. Gene expression omnibus (geo) profile and gene database, http://www.Ncbi.Nlm.Nih.Gov/sites/geo. http://www.ncbi.nlm.nih.gov/sites/geo.

33. Scripps. Biogps database of the scripps research institute, http://biogps.Org. The Scripps Research Institute.

34. Wirtz S, Neurath MF. Mouse models of inflammatory bowel disease. *Adv Drug Deliv Rev* 2007;**59**:1073-83.

35. Hibi T, Ogata H, Sakuraba A. Animal models of inflammatory bowel disease. *J Gastroenterol* 2002;**37**:409-17.

36. Dong L, Li Z, Leffler NR*, et al.* Acidosis activation of the proton-sensing GPR4 receptor stimulates vascular endothelial cell inflammatory responses revealed by transcriptome analysis. *PLoS One* 2013;**8**:e61991.

37. Sanderlin EJ, Leffler NR, Lertpiriyapong K*, et al.* GPR4 deficiency alleviates intestinal inflammation in a mouse model of acute

experimental colitis. *Biochim Biophys Acta* 2016;**1863**:569-84.

38. Solomon L, Mansor S, Mallon P*, et al.* The dextran sulphate sodium (DSS) model of colitis: An overview. Comparative Clinical Pathology: Springer London, 2010: 235-9.

39. Okayasu I, Hatakeyama S, Yamada M*, et al.* A novel method in the induction of reliable experimental acute and chronic ulcerative colitis in mice. *Gastroenterology* 1990;**98**:694-702.

40. Moore KW, de Waal Malefyt R, Coffman RL, O'Garra A. Interleukin-10 and the interleukin-10 receptor. *Annu Rev Immunol* 2001;**19**:683-765.

41. Perez-Rodriguez R, Roncero C, Olivan AM, Gonzalez MP, Oset-Gasque MJ. Signaling mechanisms of interferon gamma induced apoptosis in chromaffin cells: Involvement of nNOS, iNOS, and NfKB. *J Neurochem* 2009;**108**:1083-96.

42. Schroder K, Hertzog PJ, Ravasi T, Hume DA. Interferon-gamma: An overview of signals, mechanisms and functions. *J Leukoc Biol* 2004;**75**:163-89.

43. Seuwen; Klaus; (Basel CBEB, CH) ; Suply; Thomas; (Basel, CH) ; Wyder; Lorenza; (Basel, CH) ; Dawson King; Janet; (Basel, CH) ; Ludwig; Marie-Gabrielle; (Basel, CH) ; Mueller; Matthias; (Basel, CH) ; Nath; Puneeta; (Horsham, GB) ; Jones; Carol Elizabeth; (Horsham, GB). Inhibition of gpr4, us20100144835. In: USPTO, editor USA, 2010: 1-50.

44. P Nath JM, M Freeman, C Poll, KH Banner, T Suply, A Trifilief, and C Jones. Effect of GPR4 inhibition in a murine model of allergic asthma. D22 modulators of inflammatory pathways in airway disease. American Thoracic Society 2009 International Conference San Diego,CA, US: Am J Respir Crit Care Med, 2009: A5449.

45. Puneeta Nath CS, Mark Freeman, Chris Poll, Katharine Banner, Thomas Suply, Alexandre Triffilief, Carol Jones. Effect of GPR4 inhibition in a murine tobacco smoke model of chronic obstructive pulmonary disease. British Pharmacological Society Winter Meeting December 2008 Brighton, UK: Proceedings of the British Pharmacological Society, 2008: 017P.

46. Assassi S, Wu M, Tan FK*, et al.* Skin gene expression correlates of severity of interstitial lung disease in systemic sclerosis. *Arthritis Rheum* 2013;**65**:2917-27.

Figure 1

A

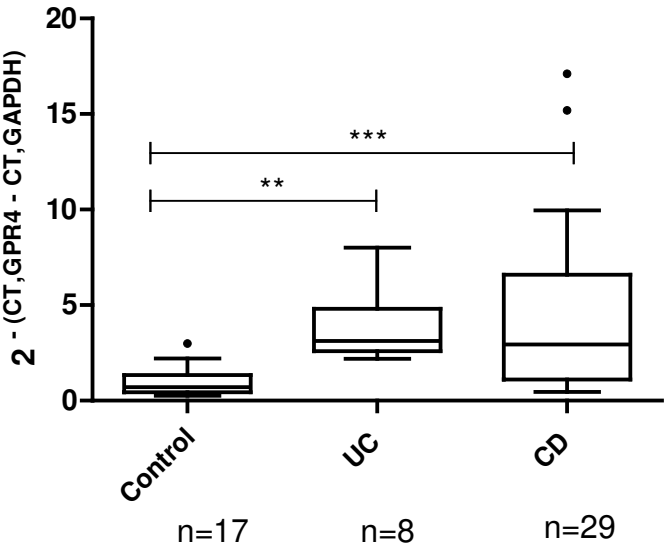
20
15
10
5
0
2 - (CT,GPR4 - CT,GAPDH)
***
**
Control
UC
CD
n=17
n=8
n=29

B

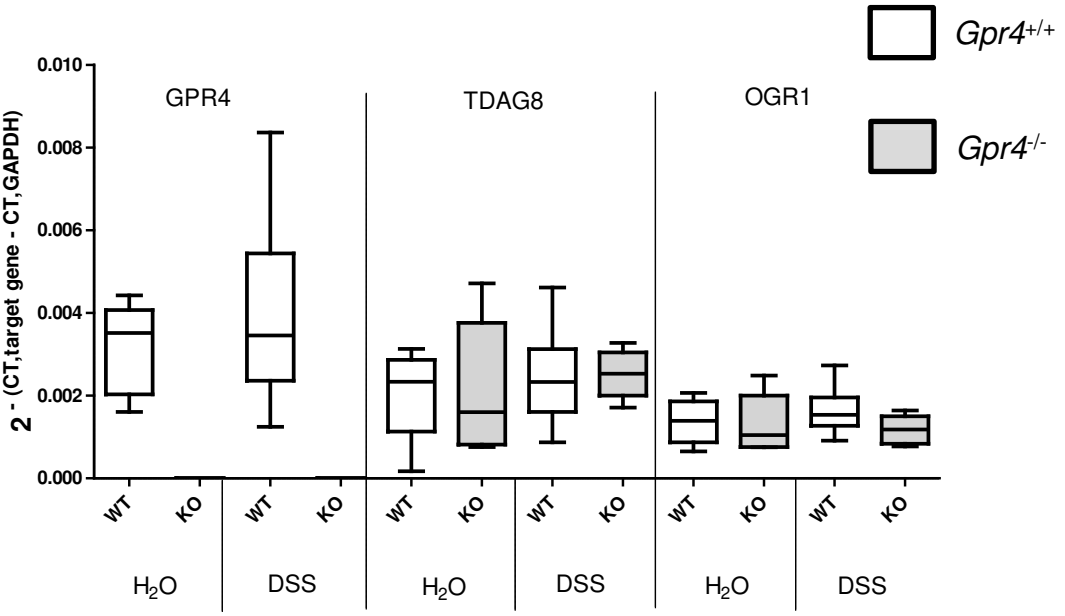
Gpr4+/+
Gpr4-/-
0.010
0.008
0.006
0.004
0.002
0.000
2 - (CT,target gene - CT,GAPDH)
GPR4
TDAG8
OGR1
WT
KO
H2O
DSS

Figure 2

A

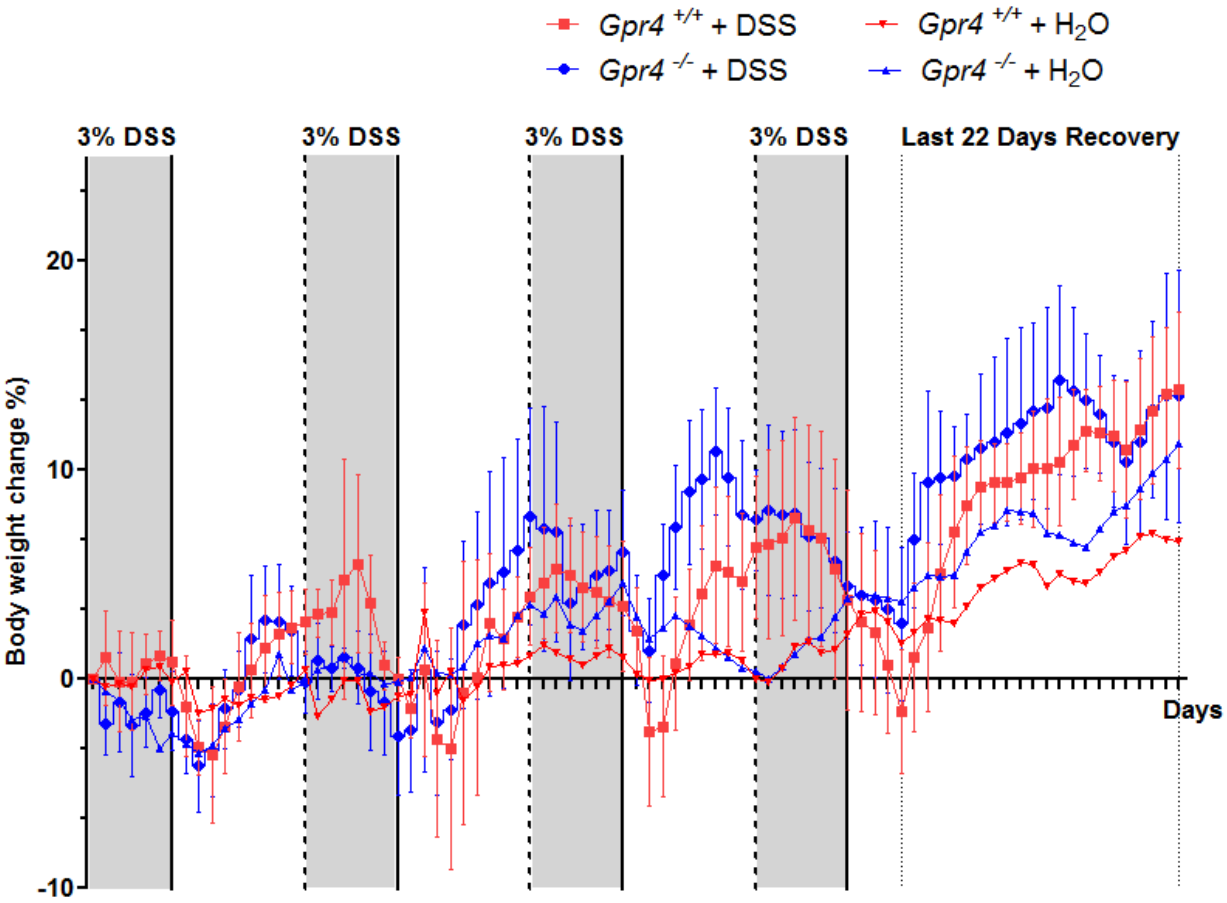
Gpr4 +/+ + DSS
Gpr4 -/- + DSS
Gpr4 +/+ + H2O
Gpr4 -/- + H2O
3% DSS
3% DSS
3% DSS
3% DSS
Last 22 Days Recovery
Body weight change %)
20
10
0
-10
Days

Figure 2 , continued

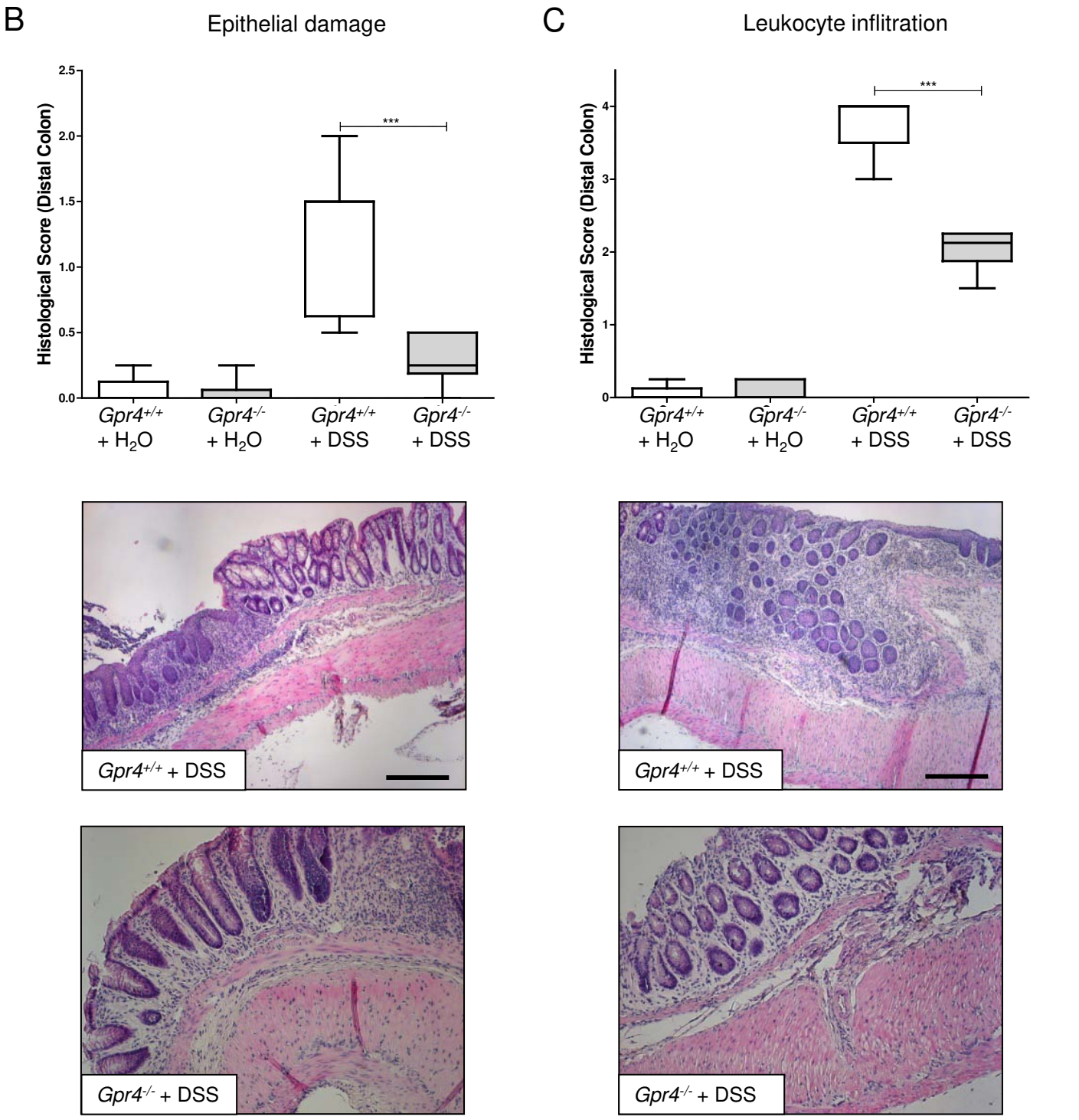

Figure 3

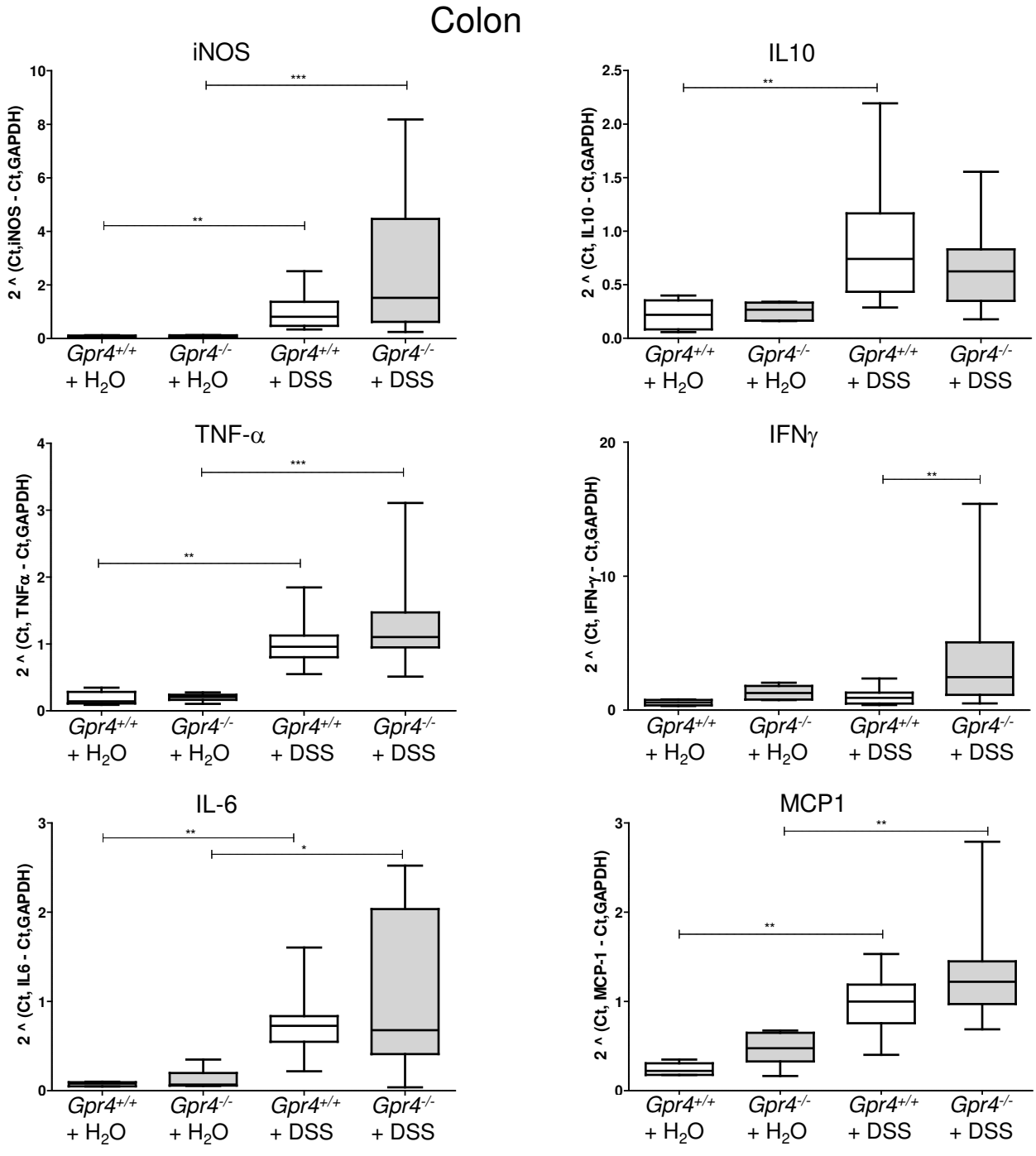
Colon
iNOS
2 ^ (Ct,iNOS - Ct,GAPDH)
IL10
2 ^ (Ct, IL10 - Ct,GAPDH)
TNF-α
2 ^ (Ct, TNFα - Ct,GAPDH)
IFNγ
2 ^ (Ct, IFN-γ - Ct,GAPDH)
IL-6
2 ^ (Ct, IL6 - Ct,GAPDH)
MCP1
2 ^ (Ct, MCP-1 - Ct,GAPDH)
Gpr4+/+ + H2O
Gpr4-/- + H2O
Gpr4+/+ + DSS
Gpr4-/- + DSS

Figure 4

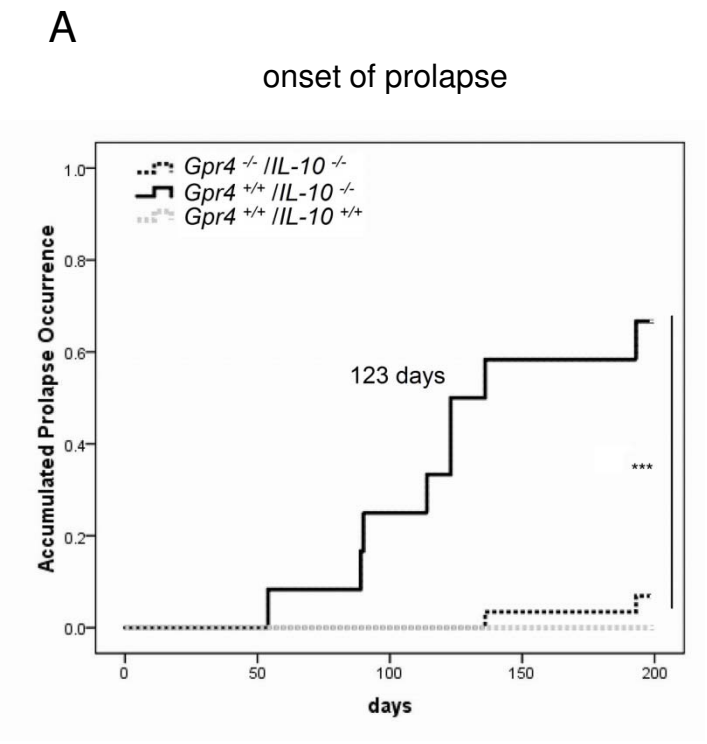
A
onset of prolapse
Gpr4 -/- /IL-10 -/-
Gpr4 +/+ /IL-10 -/-
Gpr4 +/+ /IL-10 +/+
Accumulated Prolapse Occurrence
1.0
0.8
0.6
0.4
0.2
0.0
123 days
***
0
50
100
150
200
days

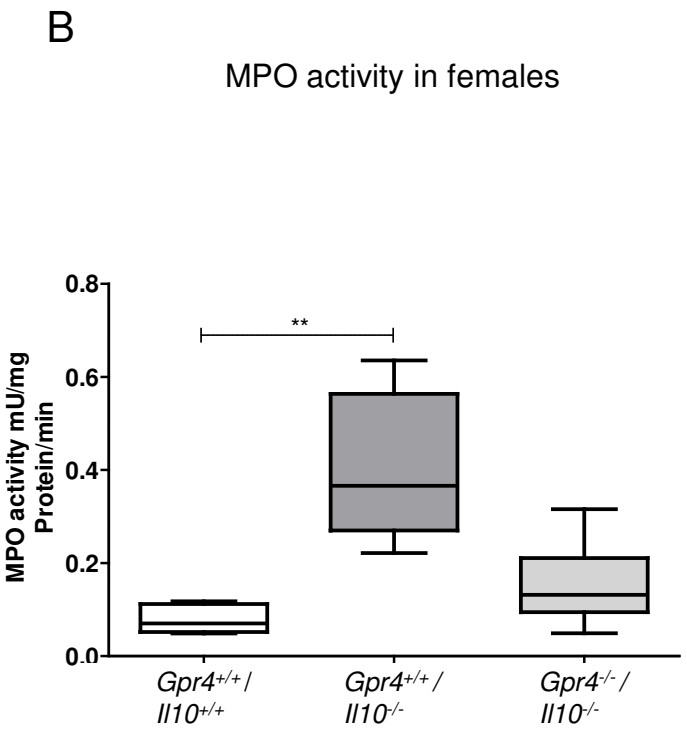
B
MPO activity in females
MPO activity mU/mg Protein/min
0.8
0.6
0.4
0.2
0.0
**
Gpr4+/+ / Il10+/+
Gpr4+/+ / Il10-/-
Gpr4-/- / Il10-/-


C
Colon length in females
Colon Length (cm)
11
10
9
8
7
6
Gpr4+/+ / Il10+/+
Gpr4+/+ / Il10-/-
Gpr4-/- / Il10-/-

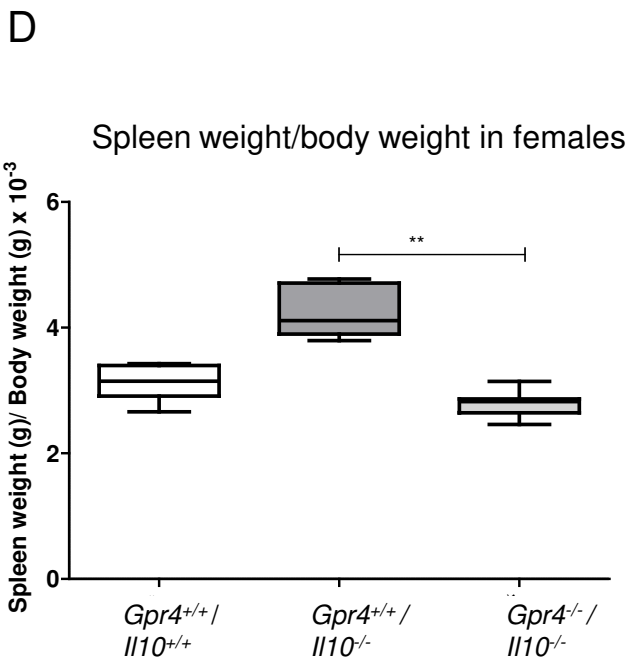
D
Spleen weight/body weight in females
Spleen weight (g)/ Body weight (g) x 10-3
6
4
2
0
**
Gpr4+/+ / Il10+/+
Gpr4+/+ / Il10-/-
Gpr4-/- / Il10-/-

Figure 5

A

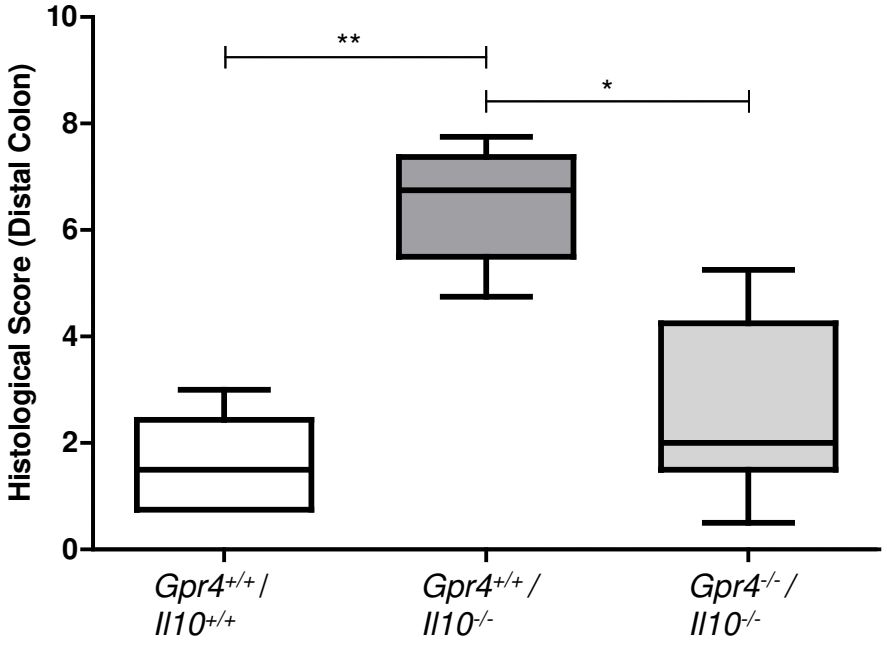

B

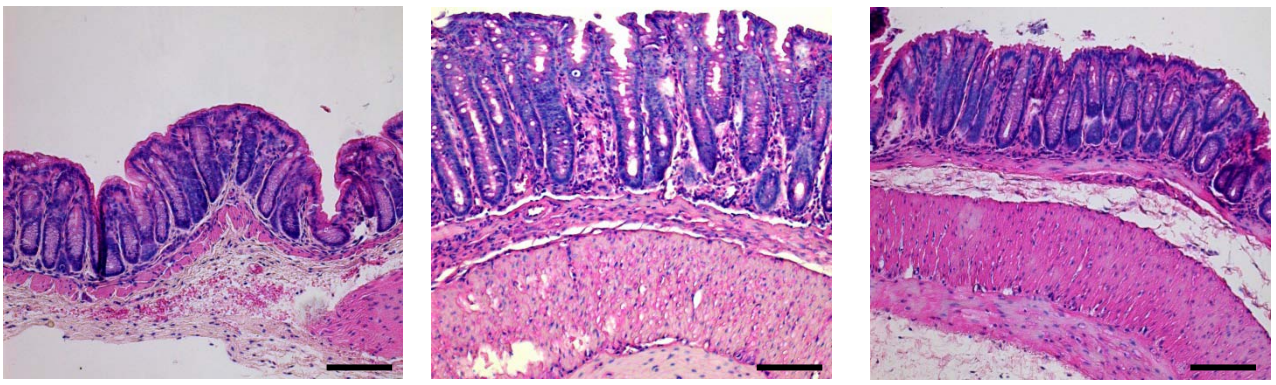

Gpr4$^{+/+}$ */IL-10*$^{+/+}$ *Gpr4*$^{+/+}$ */IL-10*$^{-/-}$ *Gpr4*$^{-/-}$ */IL-10*$^{-/-}$

Figure 6

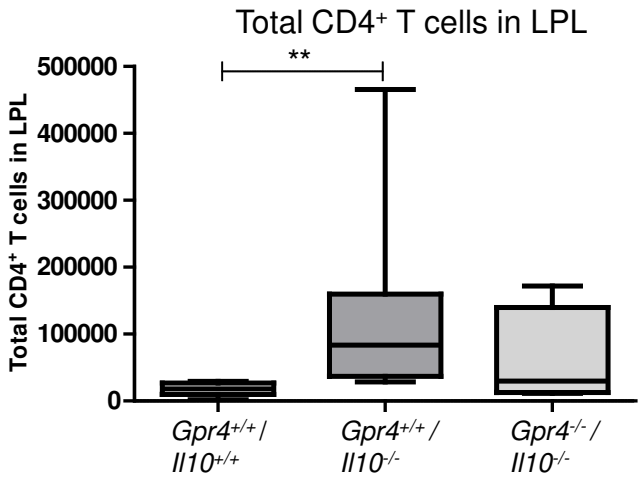
Total CD4+ T cells in LPL
Total CD4+ T cells in LPL
500000
400000
300000
200000
100000
0
**
Gpr4+/+ / Il10+/+
Gpr4+/+ / Il10-/-
Gpr4-/- / Il10-/-

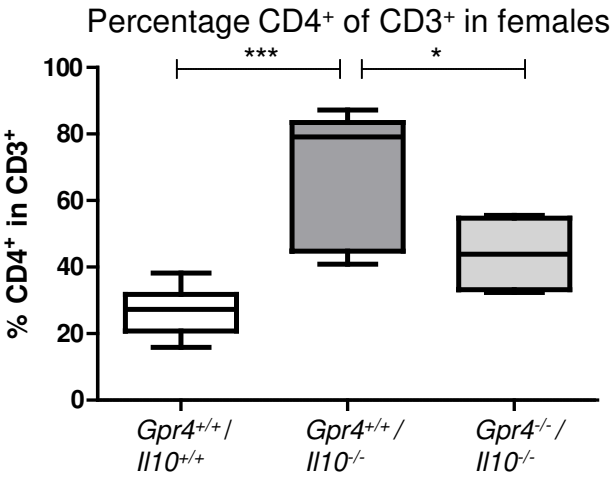
Percentage CD4+ of CD3+ in females
% CD4+ in CD3+
100
80
60
40
20
0
***
*
Gpr4+/+ / Il10+/+
Gpr4+/+ / Il10-/-
Gpr4-/- / Il10-/-

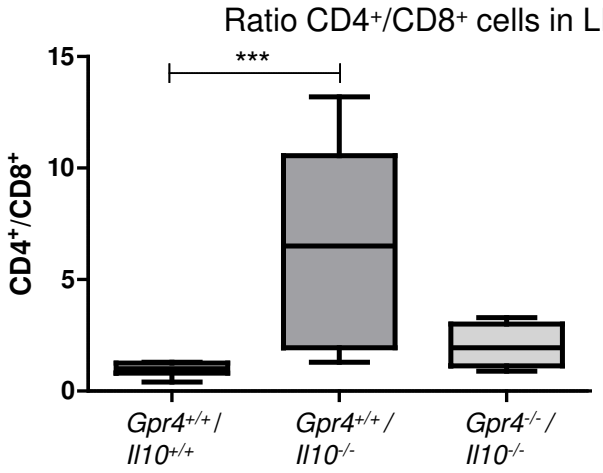
Ratio CD4+/CD8+ cells in LPL
CD4+/CD8+
15
10
5
0
***
Gpr4+/+ / Il10+/+
Gpr4+/+ / Il10-/-
Gpr4-/- / Il10-/-

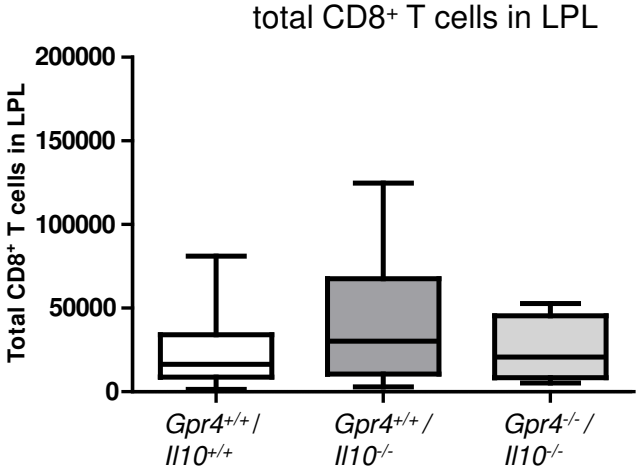
total CD8+ T cells in LPL
Total CD8+ T cells in LPL
200000
150000
100000
50000
0
Gpr4+/+ / Il10+/+
Gpr4+/+ / Il10-/-
Gpr4-/- / Il10-/-

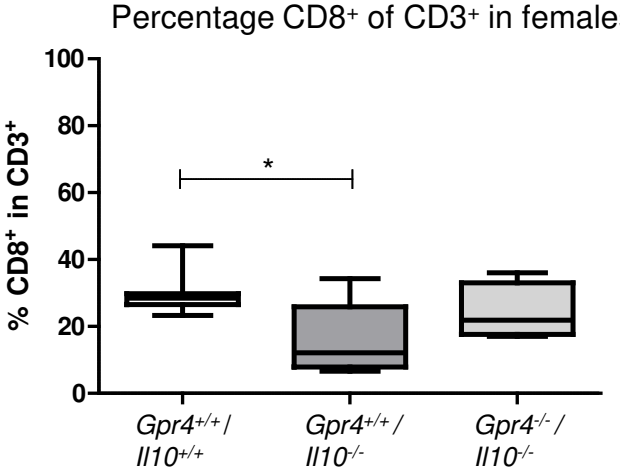
Percentage CD8+ of CD3+ in females
% CD8+ in CD3+
100
80
60
40
20
0
*
Gpr4+/+ / Il10+/+
Gpr4+/+ / Il10-/-
Gpr4-/- / Il10-/-

Figure 7

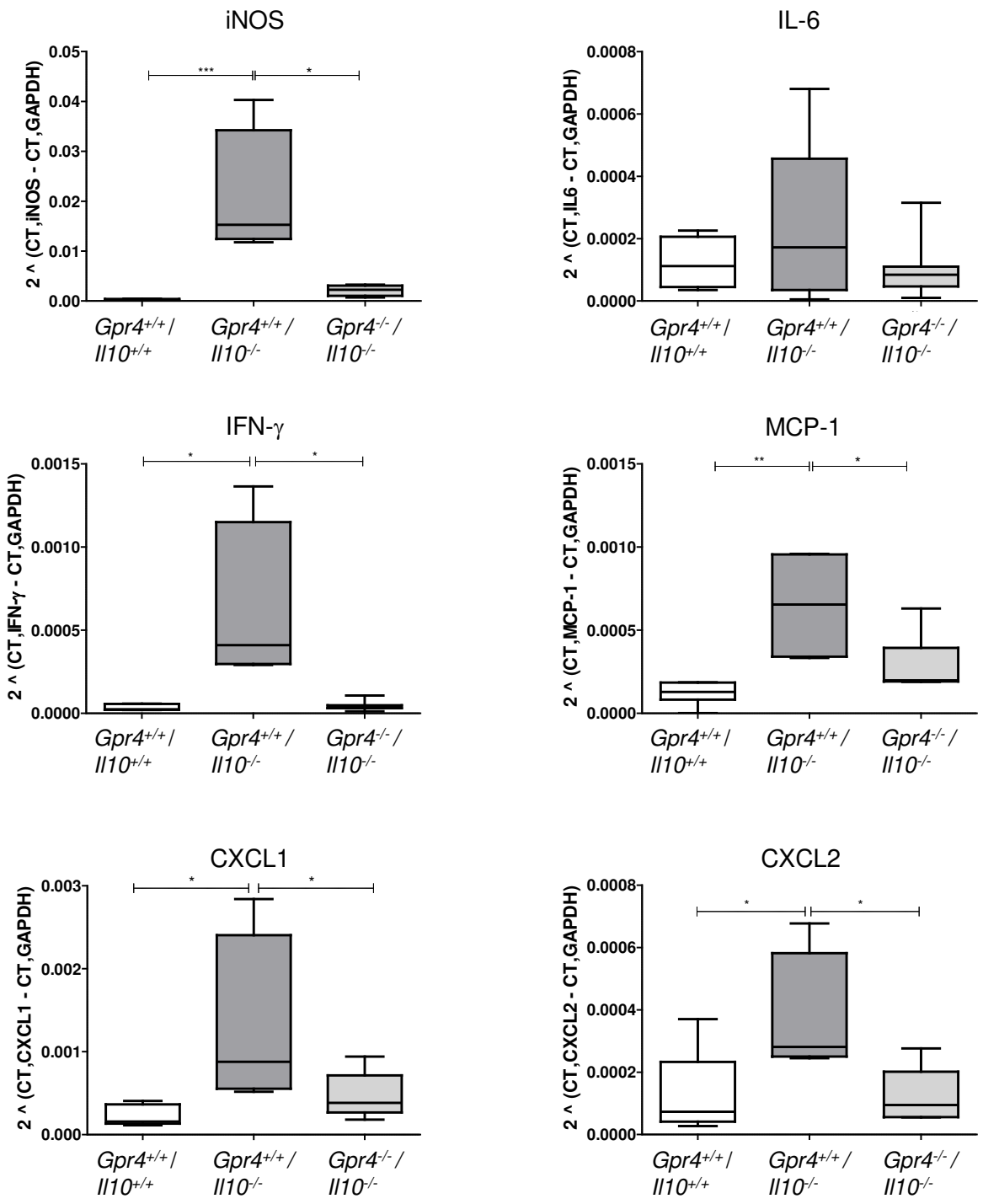
Colon
iNOS
2 ^ (CT,iNOS - CT,GAPDH)
0.05
0.04
0.03
0.02
0.01
0.00
***
*
IL-6
2 ^ (CT,IL6 - CT,GAPDH)
0.0008
0.0006
0.0004
0.0002
0.0000
IFN-γ
2 ^ (CT,IFN-γ - CT,GAPDH)
0.0015
0.0010
0.0005
0.0000
MCP-1
2 ^ (CT,MCP-1 - CT,GAPDH)
**
CXCL1
2 ^ (CT,CXCL1 - CT,GAPDH)
0.003
0.002
0.001
0.000
CXCL2
2 ^ (CT,CXCL2 - CT,GAPDH)
Gpr4+/+ / Il10+/+
Gpr4+/+ / Il10-/-
Gpr4-/- / Il10-/-

Figure 8

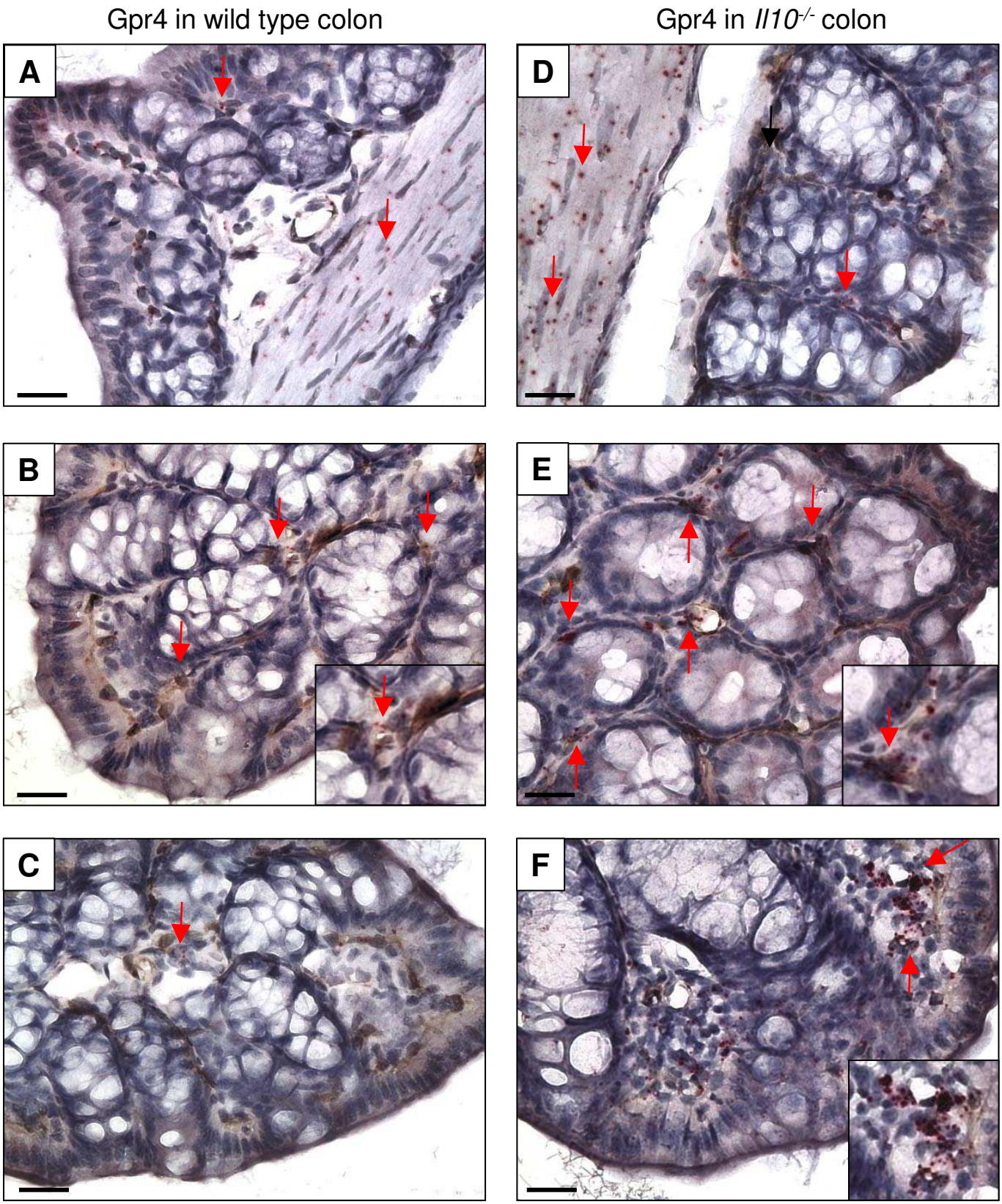

Figure 9

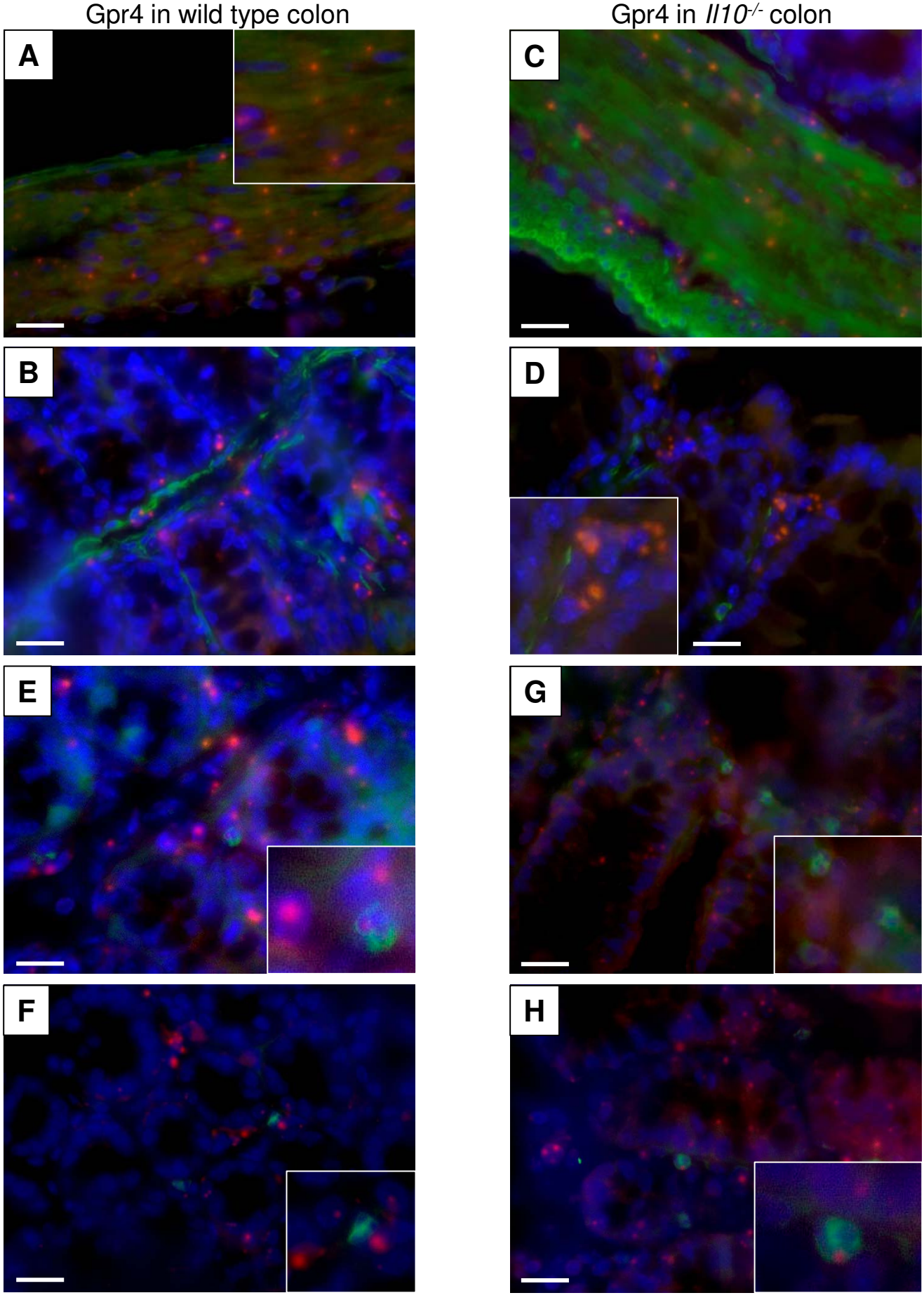

The proton-activated receptor

GPR4 modulates intestinal inflammation

Yu Wang, Cheryl de Valliere, Pedro H. Imenez Silva, Irina Leonardi, Sven Gruber, Alexandra Gerstgrasser, Achim Weber, Katharina Leucht, Lutz Wolfram, Martin Hausmann, Carsten Krieg, Koray Thomasson, Onur Boyman, Isabelle Frey-Wagner, Gerhard Rogler, Carsten A. Wagner

SUPPLEMENTS

Supplement Table 1 List of TaqMan assay probes

Gene Symbol	Gene Name	Assay ID
GAPDH	Mouse glyceraldehyde-3-phosphate dehydrogenase	Mm03302249_g1
GPR4	Mouse G protein coupled receptor 4	Mm00558777_s1
TDAG8	Mouse TDAG8 (G protein coupled receptor 65)	Mm00433695_m1
OGR1	Mouse OGR1 (G protein coupled receptor 68)	Mm00558545_s1
iNOS	Mouse nitric oxide synthase 2	Mm01309893_m1
IL-10	Mouse Interleukin 10	Mm00439615_g1
TNF-α	Mouse tumor necrosis factor alpha	Mm99999068_m1
IFN-γ	Mouse interferon gamma	Mm00801778_m1
IL-6	Mouse Interleukin 6	Mm00446190_m1
IL-18	Mouse Interleukin 18	Mm00434225_m1
MCP-1	Mouse chemokine (C-C motif) ligand 2	Mm00441242_m1
CXCL2	Mouse chemokine (C-X-C motif) ligand 2	Mm00436450_m1
CCL20	Mouse chemokine (C-C motif) ligand 20	Mm01268754_m1
CXCL1	Mouse chemokine (C-X-C motif) ligand 1	Mm04207460_m1
SELE	Mouse selectin, endothelial cell	Mm00441278_m1
VCAM1	Mouse vascular cell adhesion molecule 1	Mm01320970_m1
COX-2	Mouse prostaglandin-endoperoxide synthase 2	Mm00478374_m1

Supplement Table 2 – Summary of flow cytometry data

	Gpr4$^{+/+}$ /*Il-10*$^{+/+}$	*Gpr4*$^{+/+}$ /*Il10*$^{-/-}$	*Gpr4*$^{-/-}$ /*Il10*$^{-/-}$
Total CD45$^+$ leukocytes in LPL	311700 ± 67800	1293000 ± 545600	488200 ± 272800
% CD45$^+$ in viable single LPL	63.8 ± 8.4	83.7 ± 6.7	71.7 ± 12.2
Total CD3$^+$ T cells in LPL	77700 ± 21030	366600 ± 168000	125700 ± 64930
% CD3$^+$ in CD45$^+$	24.2 ± 3.7	29.0 ± 2.7	27.8 ± 3.0
Total Treg cells in LPL	7249 ± 1325	22140 ± 3446	16300 ± 9012
% Treg in CD4$^+$	35.9 ± 2.9	21.4 ± 2.6	24.3 ± 2.9

Supplementary Table 2

***Analysis of T Cell Subsets in Gpr4$^{+/+}$ /Il10$^{+/+}$, Gpr4$^{+/+}$ /Il10$^{-/-}$* and *Gpr4$^{-/-}$ /Il10$^{-/-}$* mice.**

Female mice were sacrificed at 80~110 days and the tissues pooled from 3 mice in each group. LPLs were stained with labeled antibodies and analyzed by flow cytometry as described in methods. Leukocytes were stained with APC conjugated anti-CD45.2 and T cell subsets identified by staining with FITC conjugated anti-CD3, PE conjugated anti-CD25, PB-Alexa 405 conjugated anti-CD4 and APC-Cy7 conjugated anti-CD8 and analyzed by flow cytometry. There were no statistics significance in total CD45$^+$ T cells in LPLs, CD45 % in viable single LPLs, total CD3$^+$ T cells in LPLs, CD3% in CD45$^+$, total Treg cells in LPLs, Treg % in CD4$^+$ between all three groups. Representative results of flow cytometric analysis of more than 5 independent experiments are shown. Data are presented as mean ± SEM.

Supplementary Figure 1

GEO profiles for GPR4 mRNA expression in various human tissues including small intestine and colon. Shown are data sets GDS3113/181558, GDS1096/211266_s_at, and GDS1096/206236_at.

Supplementary Figure 2

The total histology scores showed attenuated inflammation in *Gpr4* KO mice upon DSS colitis.

(A) The total histology scores of distal colon for *Gpr4*$^{+/+}$ + H_2O, *Gpr4*$^{-/-}$ + H_2O, *Gpr4*$^{+/+}$ + DSS and *Gpr4*$^{-/-}$ + DSS mice are shown. The total histology scores are representative for overall histology scores of distal colon (epithelial injury plus leukocytes infiltration). Data are presented as mean ± SEM; n≥ 5 per group; p <0.05 *, p <0.01 **, p <0.001 ***.

Supplementary Figure 3

Assessment of the colitis severity during DSS induced chronic colitis. Colon length, colonoscopy scores, relative spleen weight, myeloperoxidase (MPO) activity and mRNA expression profiles of cytokines were assessed in *Gpr4*$^{+/+}$ and *Gpr4*$^{-/-}$ mice treated with water or DSS, respectively. Colon length **(A)** and colonoscopy scores **(B)** showed aggravated inflammation in *Gpr4*$^{-/-}$ mice upon DSS colitis. *Gpr4*$^{+/+}$ and *Gpr4* $^{-/-}$ mice showed similar relative spleen weight (spleen weight (g)/ Body weight (g) x 10^{-3}) **(C)** and MPO activity in colonic tissue **(D)** upon DSS treatment. **(E)** The mRNA expression levels of iNOS, IL-10, TNF-α, IFN-γ, IL-6, IL-18 and MCP-1 in mesenteric lymph nodes from *Gpr4*$^{-/-}$ mice and *Gpr4*$^{+/+}$ mice with or without administration of DSS were not changed. For quantification, values are mean ± SEM; n ≥ 5 per group; P < 0.05 *, P < 0.01 **, P < 0.001 ***. Data are representative of 3 independent experiments.

Supplementary Figure 4

Less histological damage in *Gpr4*$^{-/-}$ /*Il10*$^{-/-}$ female mice.

H&E stained sections showed the significant difference in the damage of epithelial integrity and intensity of the leukocyte infiltration into inflamed sites. The same sections are shown in higher magnifications in figure 5. Scale bar 300 μm.

Supplementary Figure 5

Development of IBD and progression of prolapse differ between *Gpr4*$^{-/-}$ /*Il10*$^{-/-}$ and *Gpr4*$^{+/+}$ /*Il10*$^{-/-}$ *male* mice.

(A) Kaplan-Meier prolapse-free survival curve showed delayed onset and

progression of prolapse in male *Gpr4*$^{-/-}$ /*Il10*$^{-/-}$ mice relative to male *Gpr4*$^{+/+}$ /*Il10*$^{-/-}$ mice (estimated median prolapse-free survival time, >200 days vs. 161 days, ** p=0.007, log rank (Mantel-Cox) test). Black dotted lines, *Gpr4*$^{-/-}$ /*Il10*$^{-/-}$ mice (24.4% prolapses, n=41, male); black solid line, *Gpr4*$^{+/+}$ /*Il10*$^{-/-}$ mice (52.0% prolapses, n=25, male); grey dotted lines, *Gpr4*$^{+/+}$ /*Il10*$^{+/+}$ mice (0% prolapses, n=26, male). Comparison of MPO activity in colon tissue **(B),** colon length **(C)** and relative spleen weight **(D)** showed attenuated colitis in male *Gpr4*$^{-/-}$ /*Il10*$^{-/-}$ mice (not significant but MPO activity, p<0.05 *, Kruskal-Wallis one-way ANOVA followed by Dunn's multiple-comparison test).

Supplementary Figure 6

***Reduction* of histology scores in *Gpr4*$^{-/-}$ /*Il10*$^{-/-}$ male mice.**

(A) The total histology scores of distal colon for male *Gpr4*$^{-/-}$ /*Il10*$^{-/-}$, *Gpr4*$^{+/+}$ /*Il10*$^{-/-}$ and *Gpr4*$^{+/+}$ /*Il10*$^{+/+}$ mice at 80 days of age were shown, indicating reduced inflammation in *Gpr4*$^{-/-}$ /*Il10*$^{-/-}$ mice (p<0.05, *Gpr4*$^{-/-}$ /*Il10*$^{-/-}$ compared to *Gpr4*$^{+/+}$ /*Il10*$^{-/-}$*)*. The total histology scores are representative for overall histology scores of distal colon (epithelial injury plus leukocytes infiltration). Data are presented as mean ± SEM; n ≥ 5 per group; p <0.05 *, p <0.01 **, p <0.001 ***. **(B)** H&E staining sections showed the significant difference in the damage of epithelial integrity and intensity of the leukocyte infiltration into inflamed sites. Scale bar 100 μm.

Supplementary Figure 7

Suppression of IFN-γ-producing CD4$^+$ T helper cells in *Gpr4*$^{-/-}$ /*Il10*$^{-/-}$ mice. Dot plots of the expression of CD4$^+$ vs. CD8$^+$ in LPLs isolated from female *Gpr4*$^{-/-}$ /*Il10*$^{-/-}$, *Gpr4*$^{+/+}$ /*Il10*$^{-/-}$ and *Gpr4*$^{+/+}$ /*Il10*$^{+/+}$ mice are shown. LPLs were isolated and stained with anti-CD4 conjugated to PB-Alexa 405 and with anti-CD8 conjugated to APC-Cy7 and analyzed by flow cytometry.

Representative flow cytometry results from more than 5 qualitatively similar experiments are shown; isolated LPLs from 3 female mice were pooled in each group.

Supplementary Figure 8

Analysis of mRNA expression profiles of cytokines in colon and mesenteric lymph nodes in female *Gpr4*$^{-/-}$ /*Il10*$^{-/-}$ and *Gpr4*$^{+/+}$ /*Il-10*$^{-/-}$ mice. **(A)** The mRNA expression profiles of IL-18, SELE, CCL20, VCAM-1, and COX-2 were analyzed by semi-quantitative RT-qPCR in colon tissue from of all three female strains (*Gpr4*$^{-/-}$ /*Il10*$^{-/-}$, *Gpr4*$^{+/+}$ /*Il10*$^{-/-}$ and *Gpr4*$^{+/+}$ /*Il10*$^{+/+}$ mice). **(B)** mRNA expression profiles of iNOS, TNF-α, IFN-γ, IL-6, CXCL1, CXCL2, CCL20, MCP-1, VCAm-1, COX-2 in lymph nodes from same animals. ($P<$ 0.05*, Kruskal-Wallis one-way ANOVA followed by Dunn's multiple-comparison test). Data are presented as relative expression normalized to the house-keeping gene GAPDH, n = 6-9 mice per group. Data are presented as mean ± SEM.

Supplementary Figure 9

The mRNA expression profile of cytokines in colon (A) and mesenteric lymph nodes (B) between *Gpr4*$^{-/-}$ /*Il10*$^{-/-}$ and *Gpr4*$^{+/+}$ /*Il10*$^{-/-}$ *male* mice.

iNOS, TNF-α, IFN-γ, IL-6, MCP-1, IL-18, CXCL2, CCL20, CXCL1, SELE, VCAM1 and COX-2 of all three male strains (*Gpr4*$^{-/-}$ /*Il10*$^{-/-}$, *Gpr4*$^{+/+}$ /*Il10*$^{-/-}$ and *Gpr4*$^{+/+}$ /*Il10*$^{+/+}$ mice) were determined by real time RT-PCR Taqman assay. Data represent copies of cytokine mRNA/GAPDH and mRNA amplification was representative of 6~9 mice per group. The homogenate of each mouse was tested in triplicates. Data are presented as mean ± SEM; $p < 0.05$ *, $p < 0.01$ **, $p < 0.001$ ***.

Supplementary Figure 10

Localization of Gpr4 mRNA in murine proximal colon of *Gpr4*$^{-/-}$ mice

Chromogenic in-situ hybridization of Gpr4 mRNA (brown dots) in murine proximal colon using RNAscope. **(A-B)** Wildtype colon, **(C,-D)** Colon from *Il10*$^{-/-}$. Scale bar 50 μm.

Supplementary Figure 11

Controls for localization of Gpr4 mRNA in murine proximal colon of *Gpr4*$^{-/-}$ mice

(A,B) In-situ hybridization of Gpr4 mRNA in the proximal colon of Gpr4-/- mice. No signal was detected. **(C)** To confirm the function of the RNAscope, mRNA of the ubiquitously expressed Peptidyl-prolyl cis-trans isomerase B (*Pipb*) was tested and detected. Scale bar 50 μm.

Supplementary Figure 1

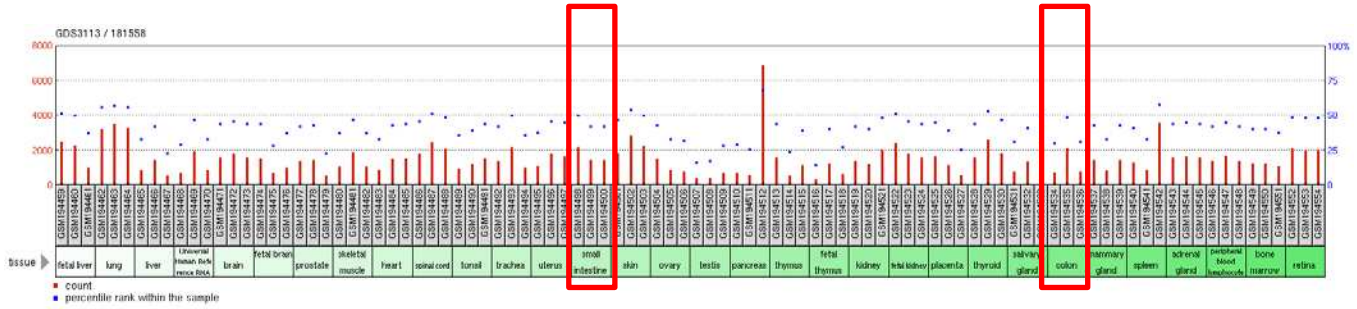

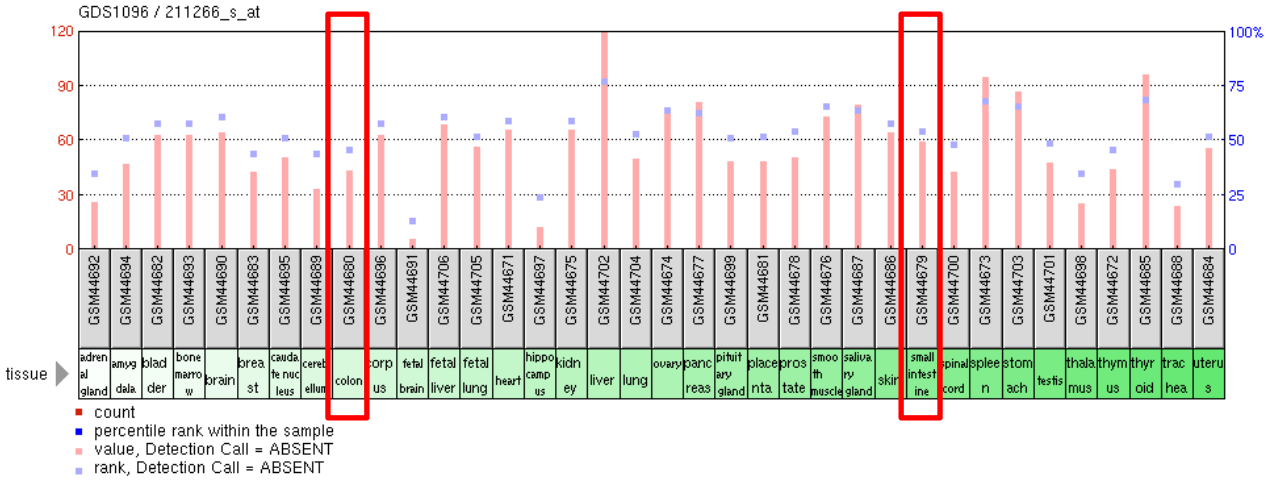

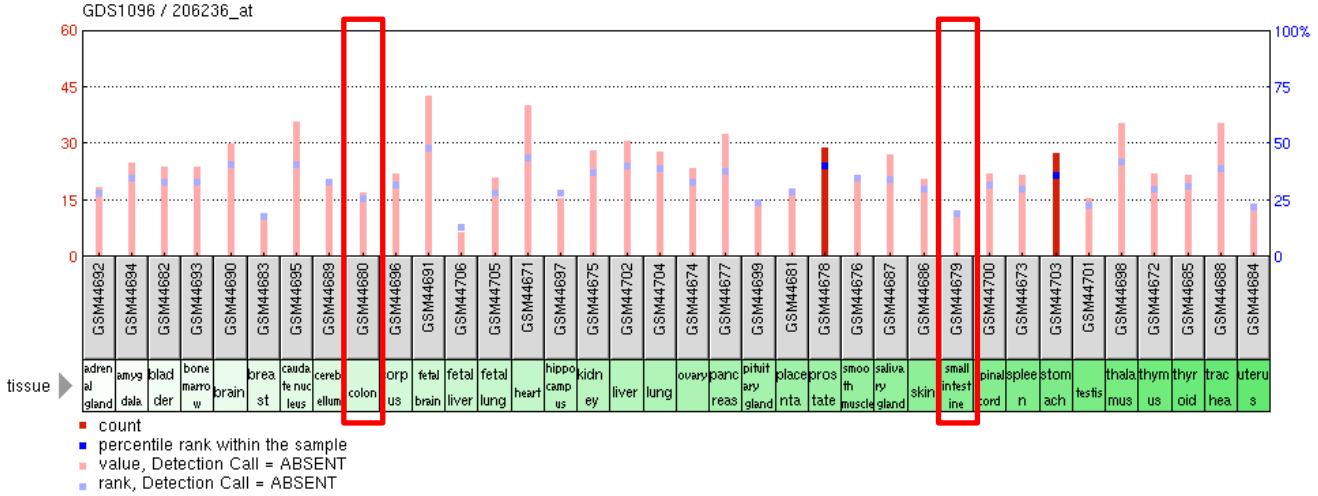

Supplementary Figure 2

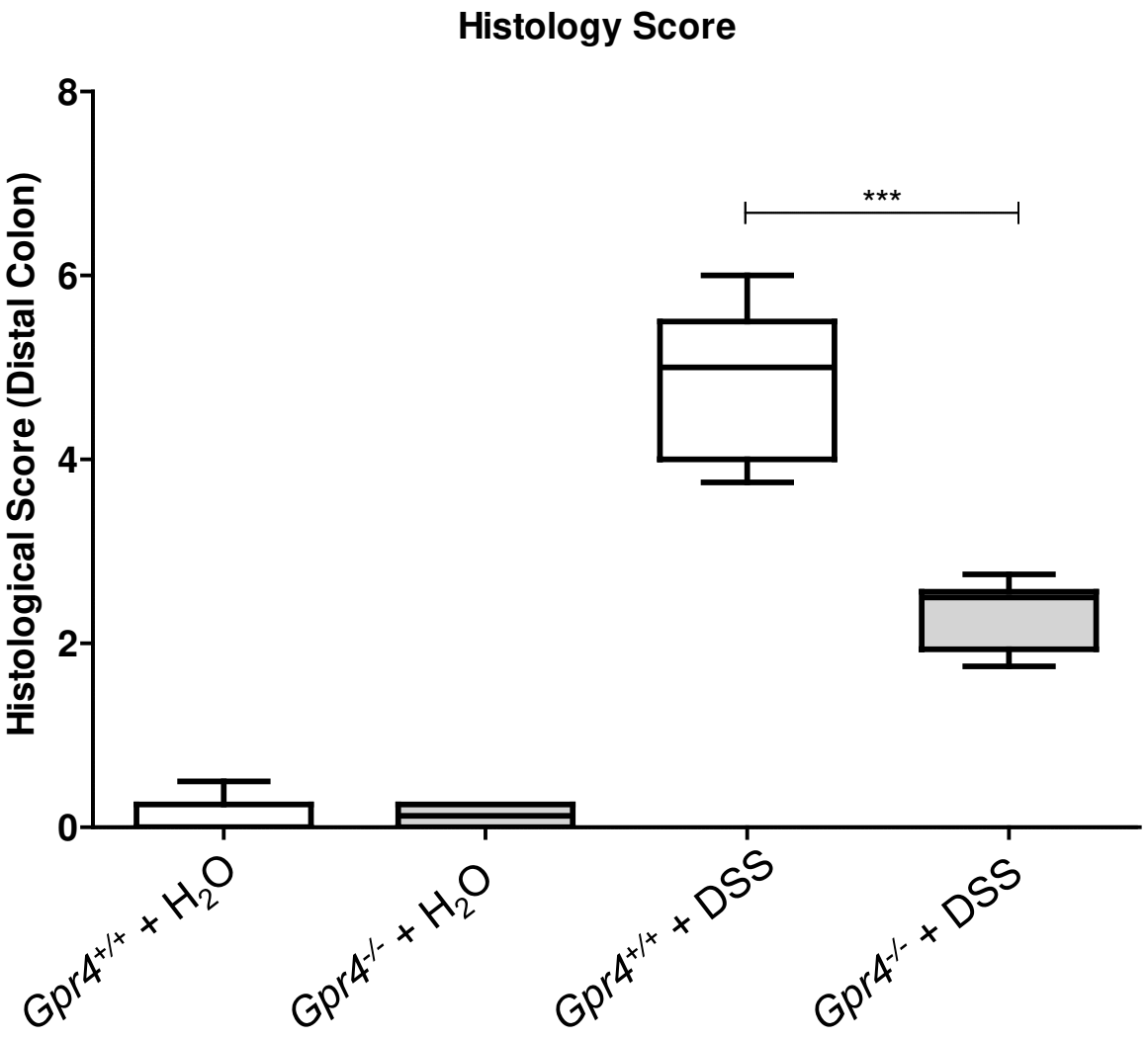

Supplementary figure 3

A

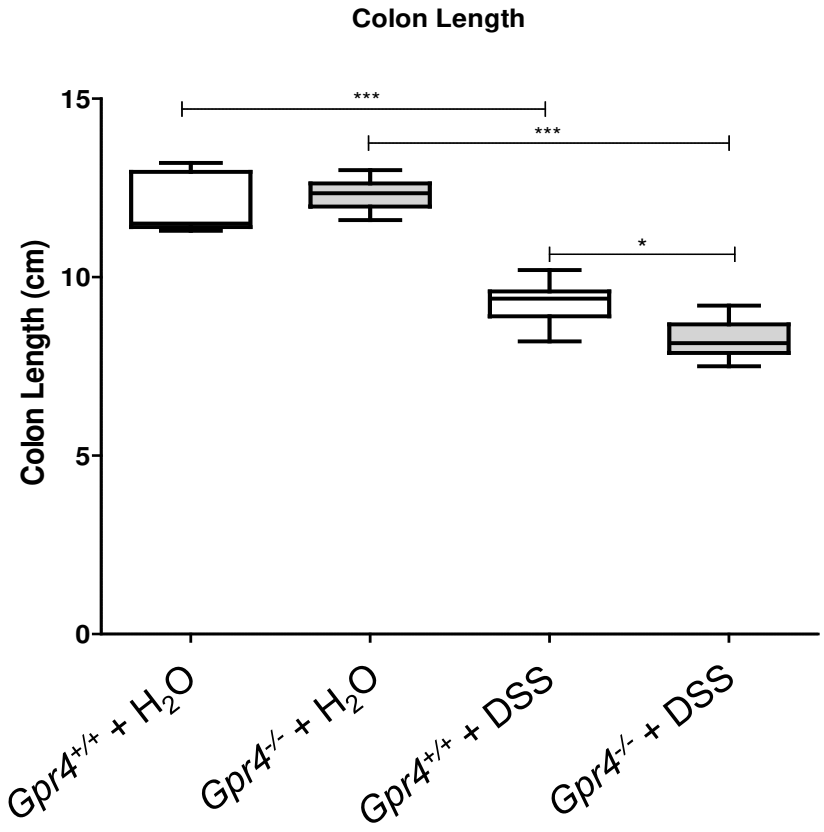

B

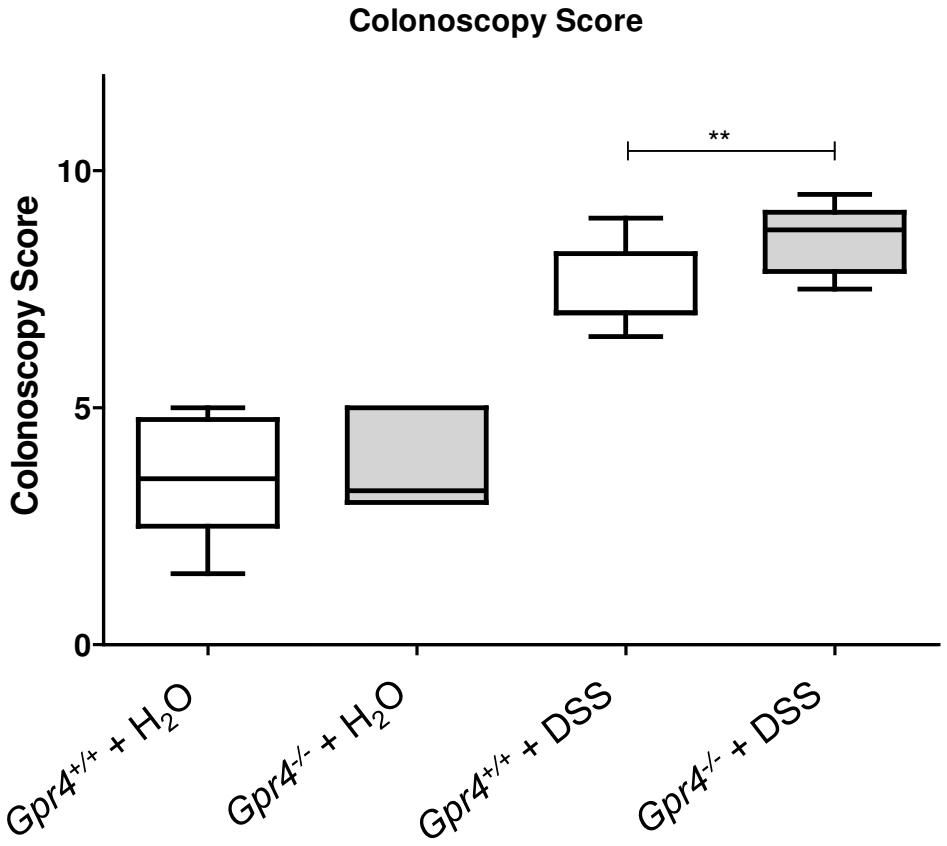

Supplementary figure 3 continued

C

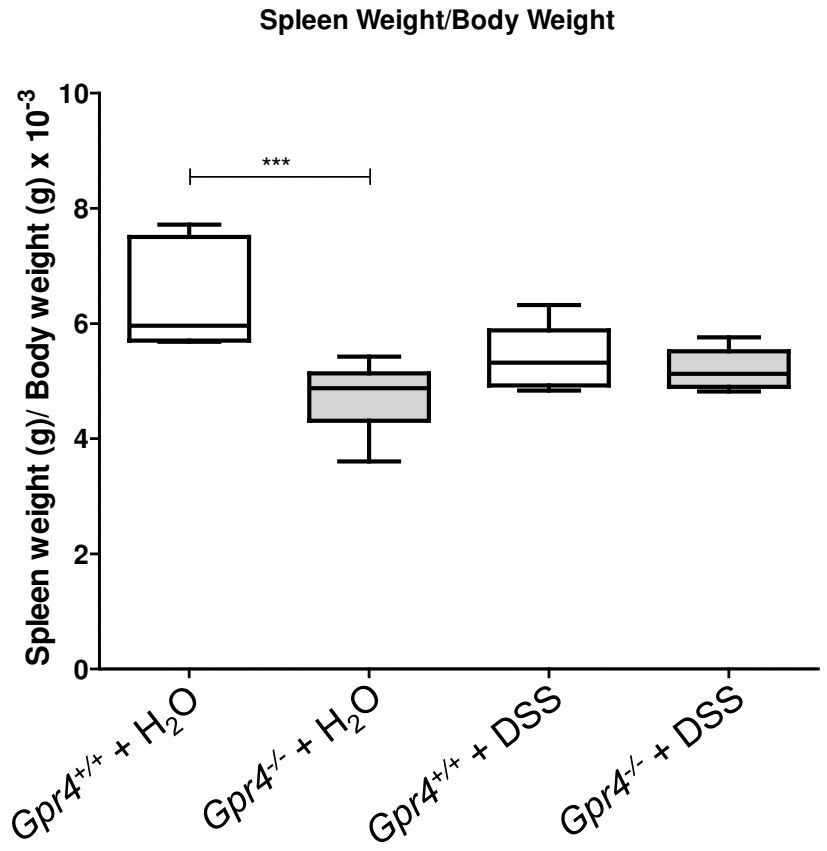

D

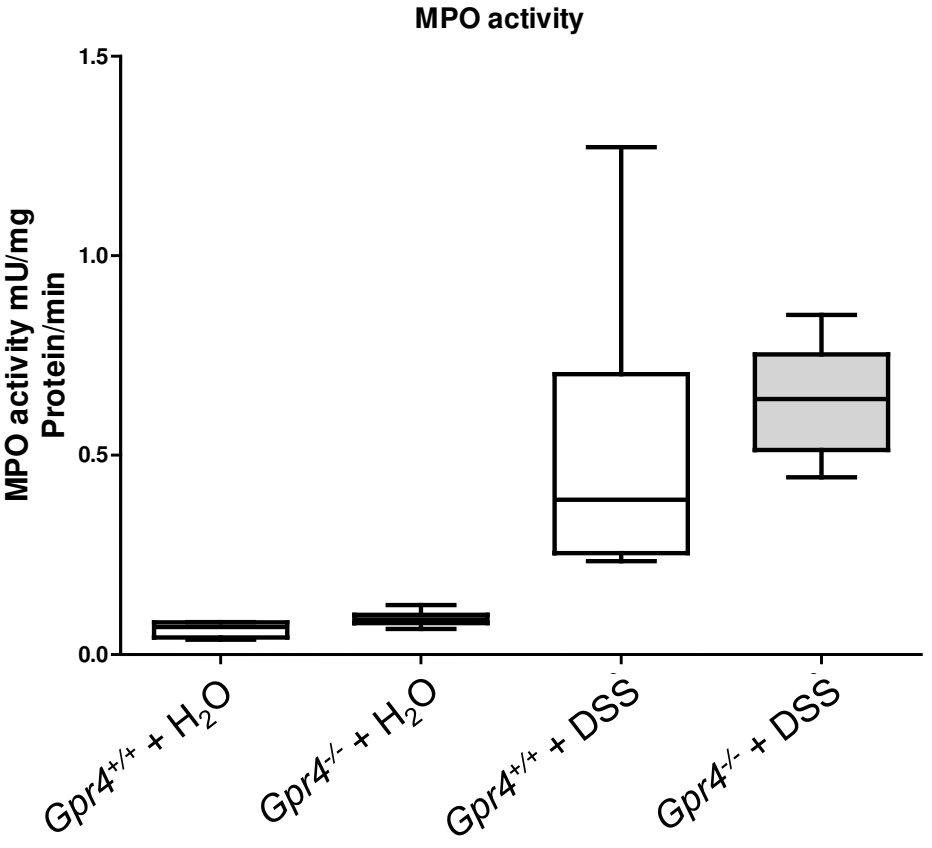

Supplementary figure 3 continued

E

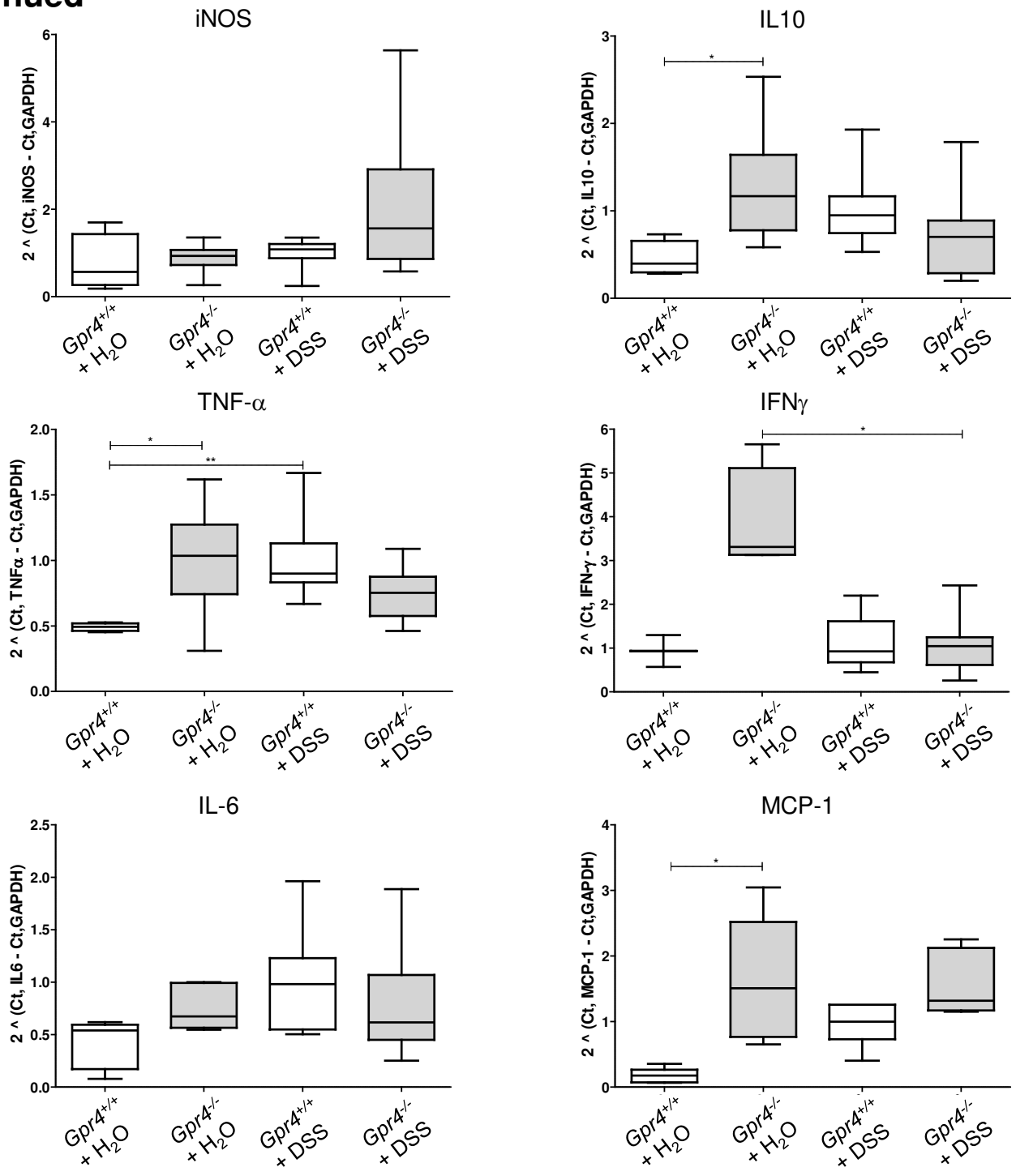

Supplementary Figure 4

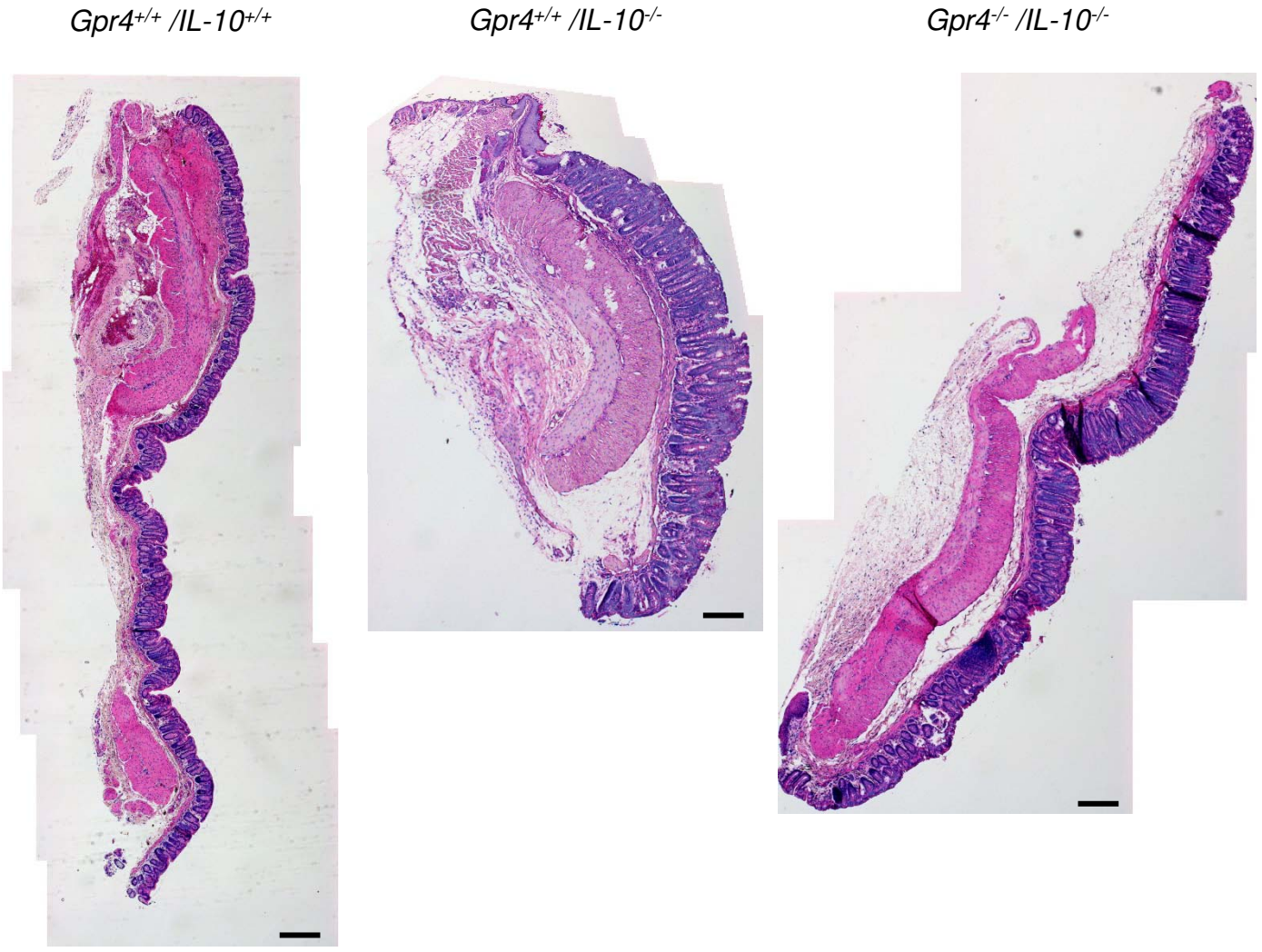

Supplementary Figure 5

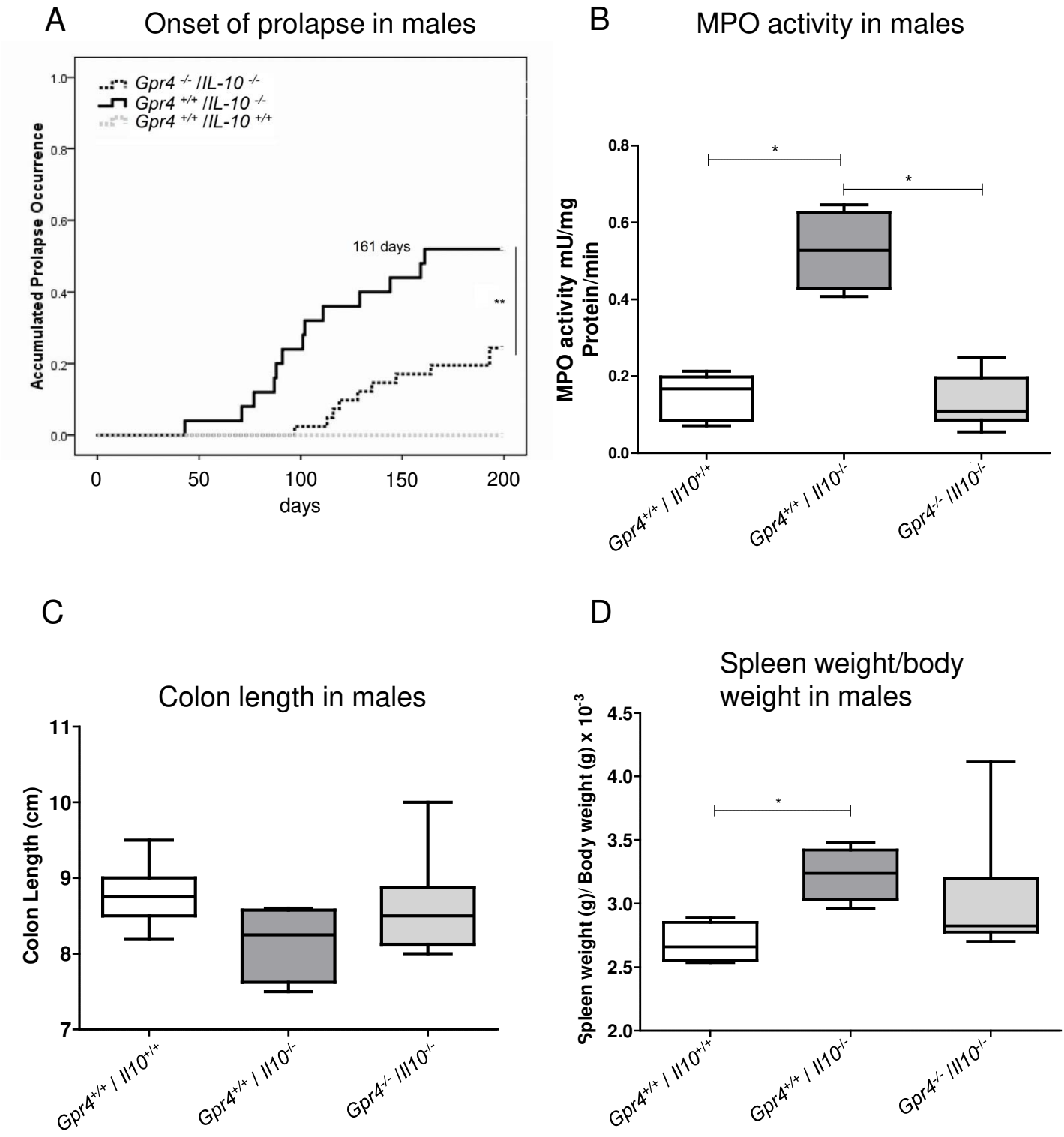

Supplementary Figure 6

A

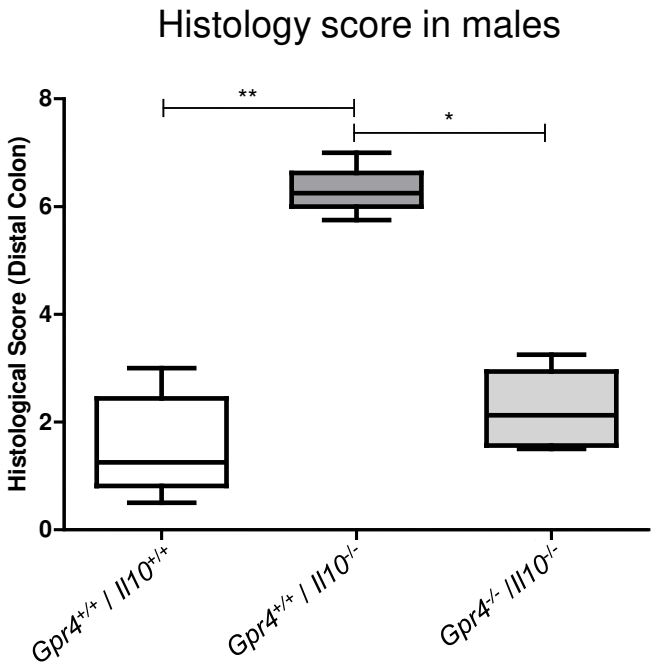

B

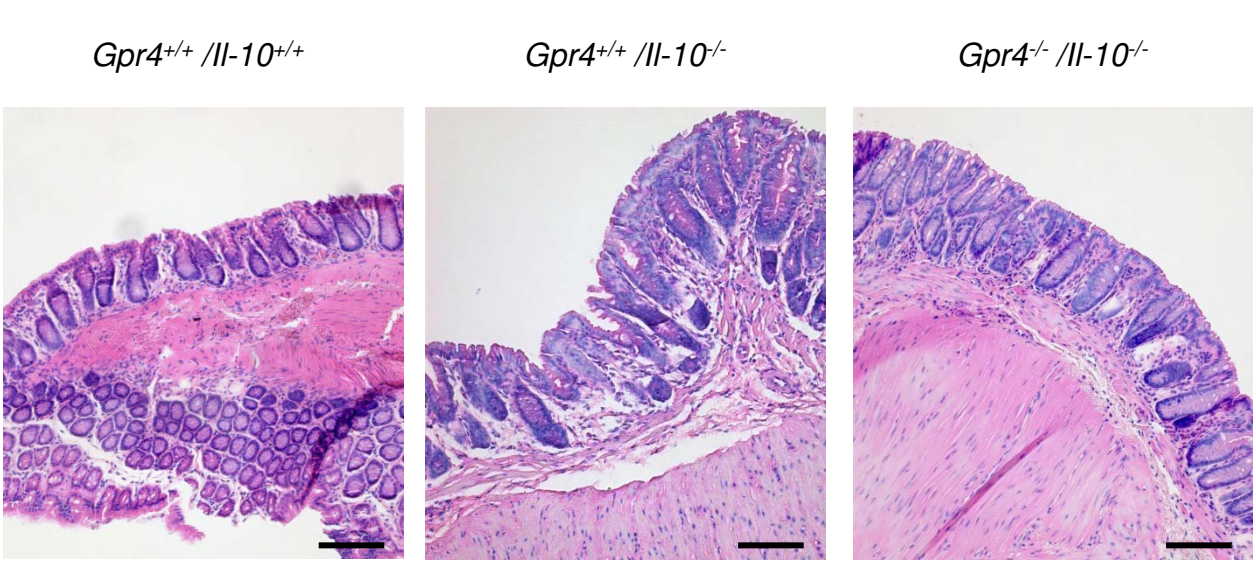

Supplementary Figure 7

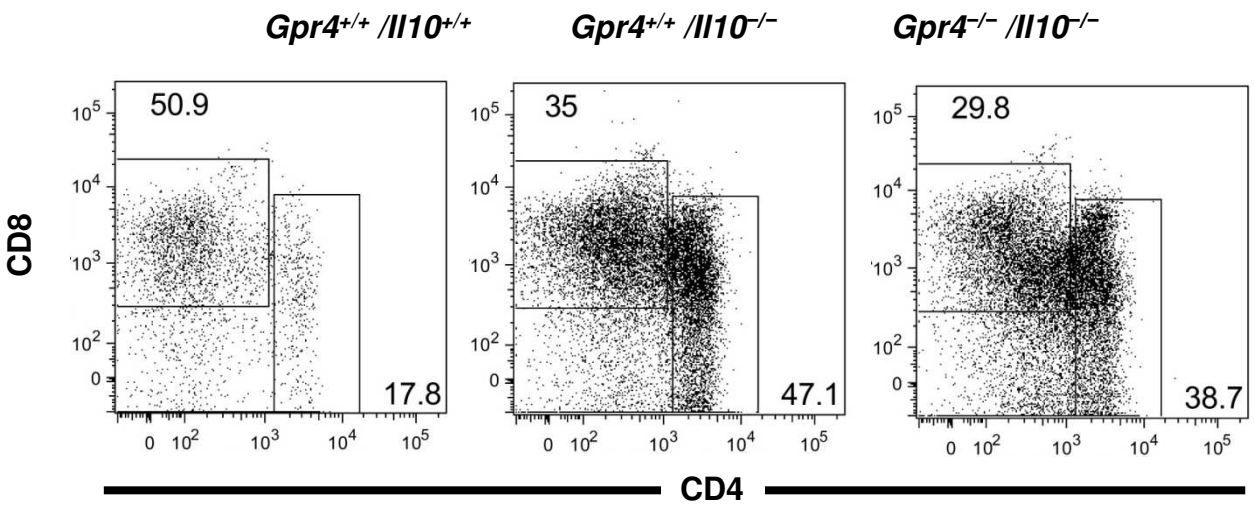

Supplementary figure 8

Colon, females

A

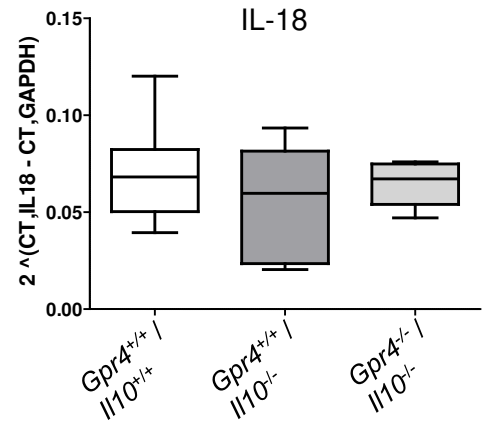

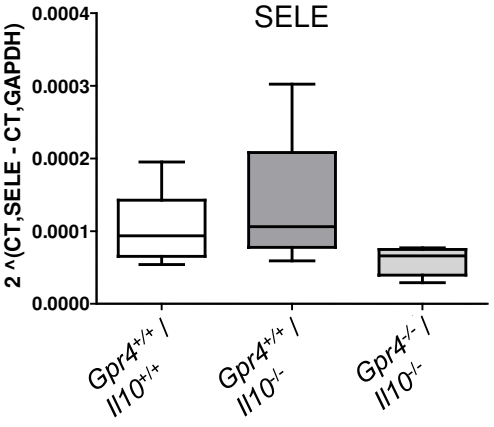

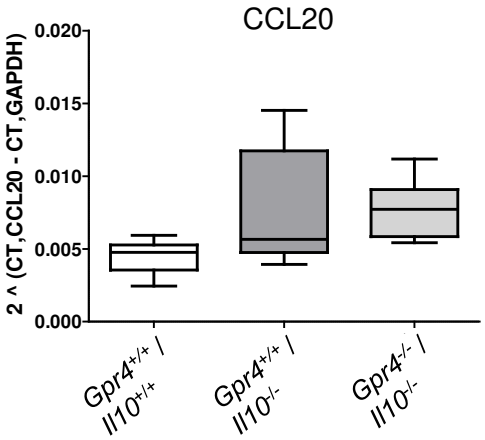

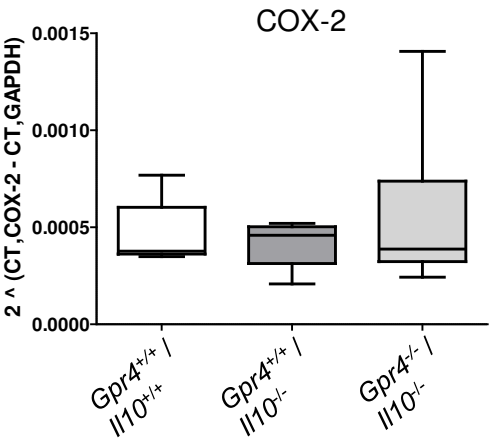

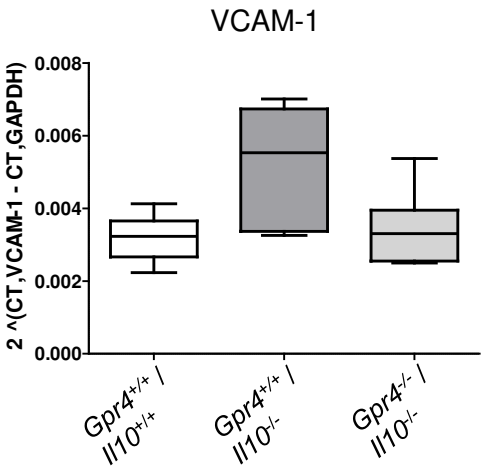

Supplementary figure 8 continued

lymph nodes, females

B

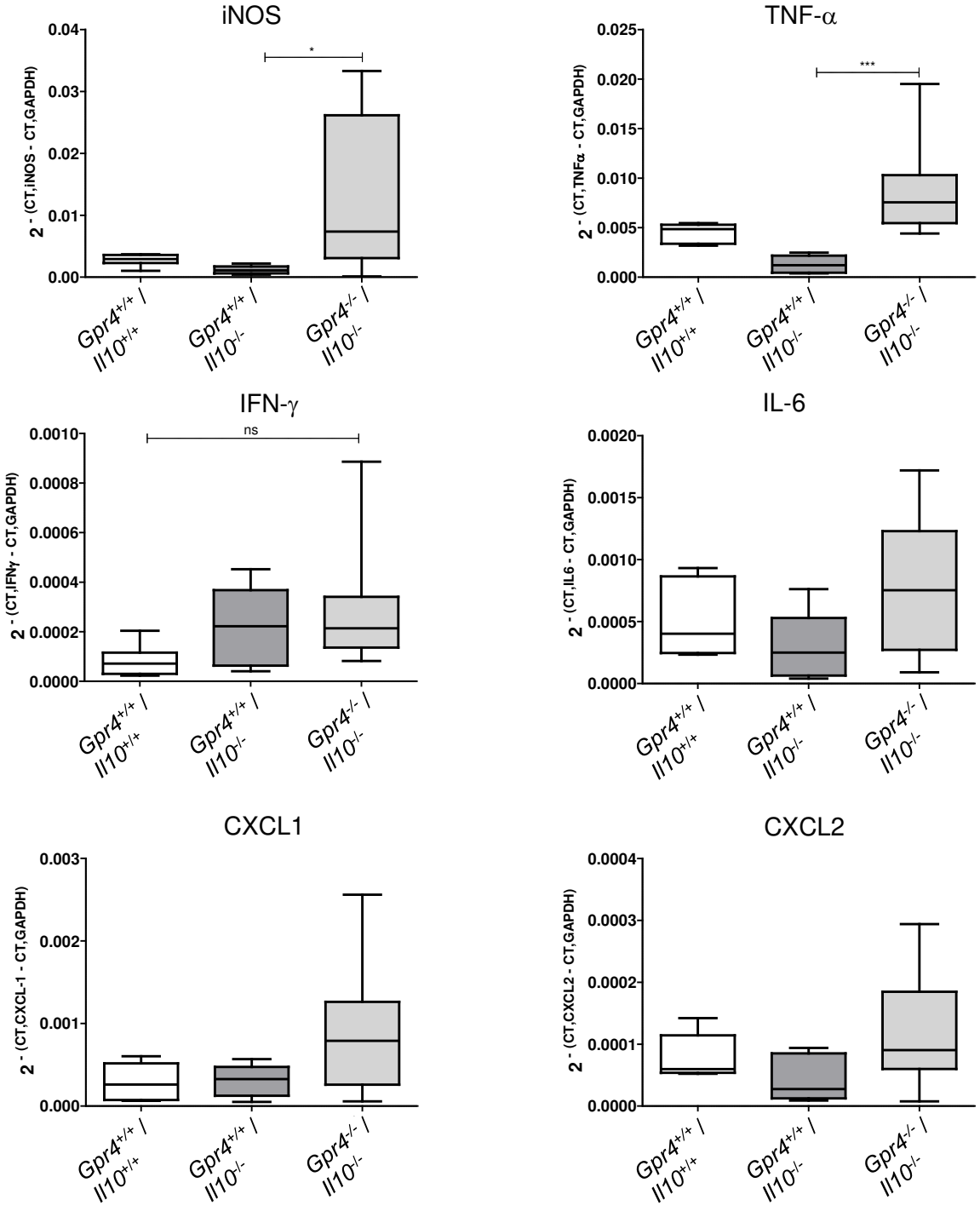

Supplementary figure 8 continued

lymph nodes, females

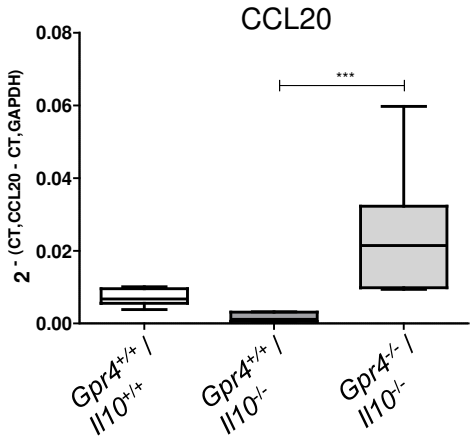

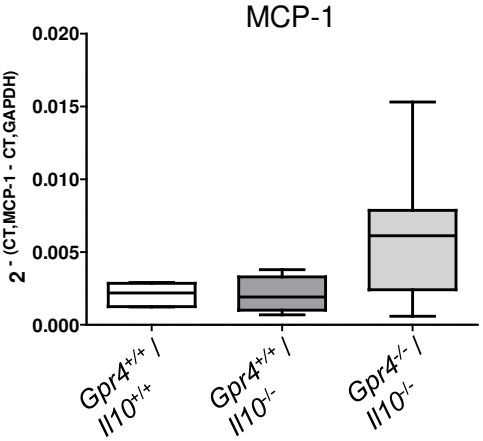

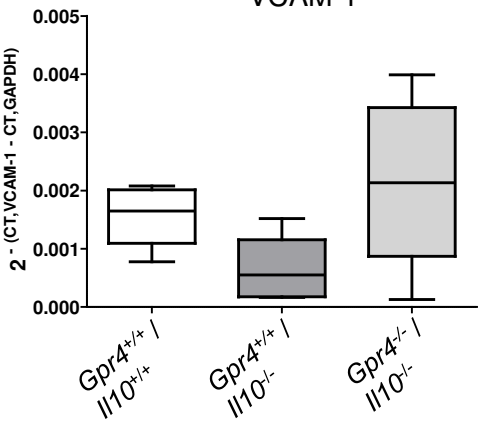

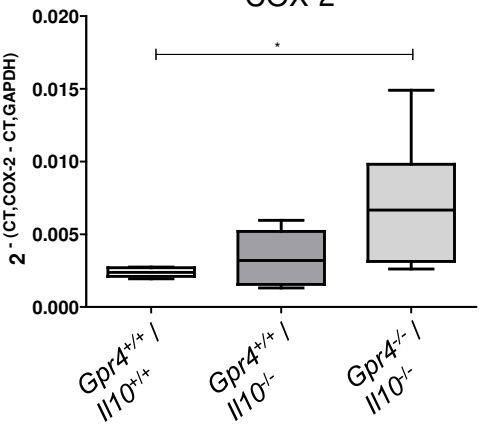

Supplementary Figure 9 Colon, males

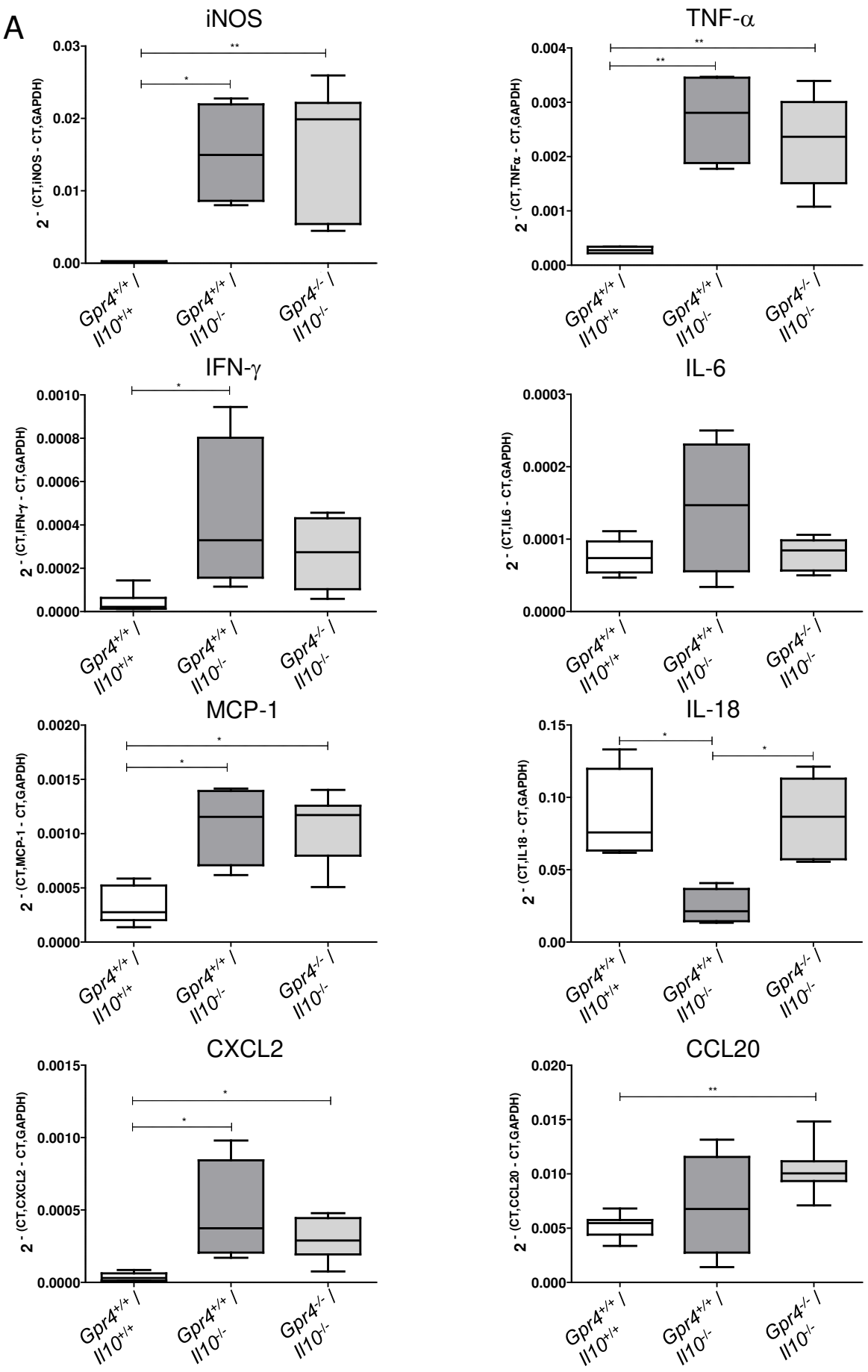

Supplementary Figure 9 continued

Colon, males

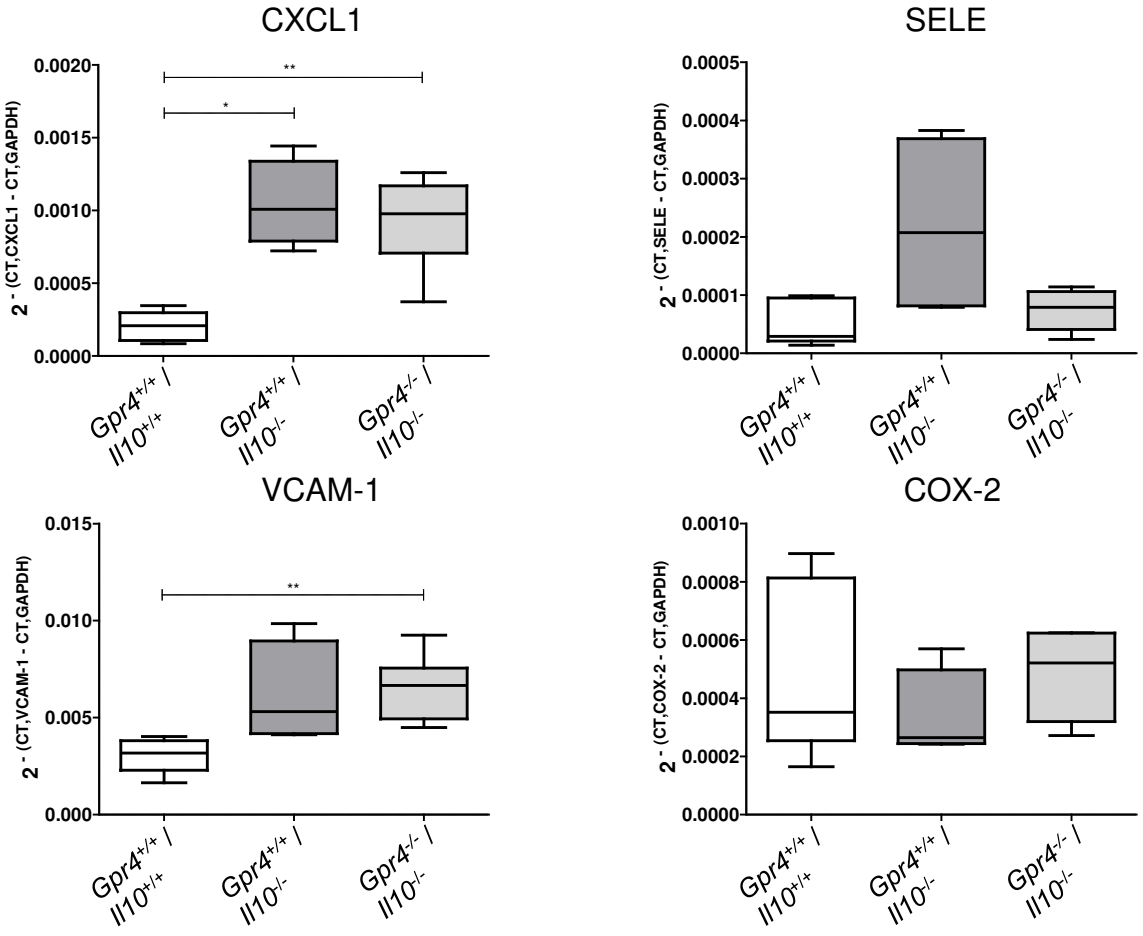

Supplementary Figure 9 continued

Lymph nodes, males

B

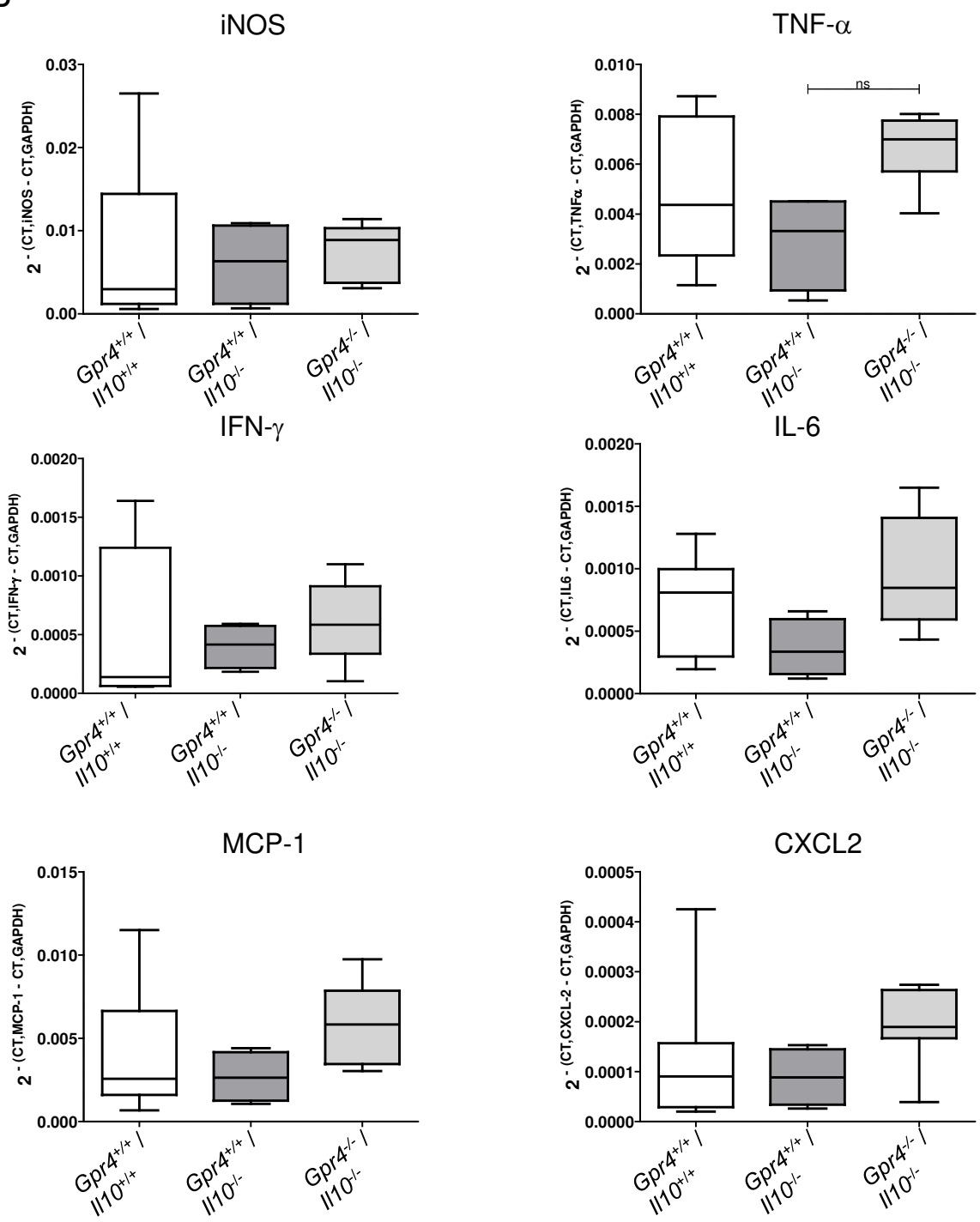

Supplementary Figure 9 continued

Lymph nodes, males

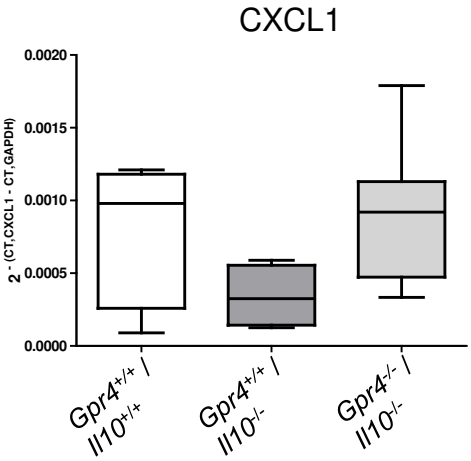

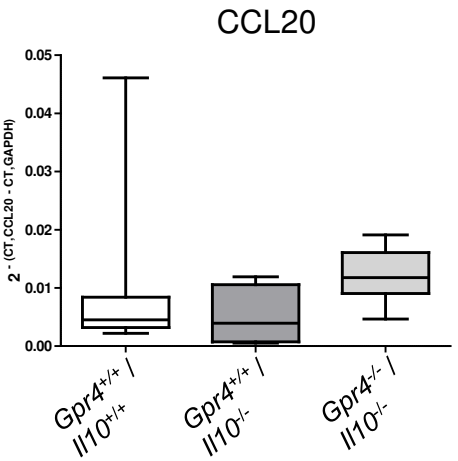

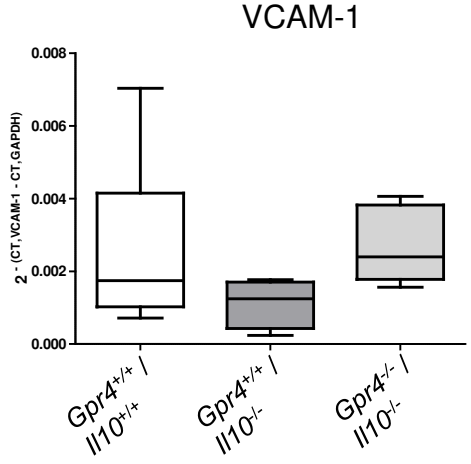

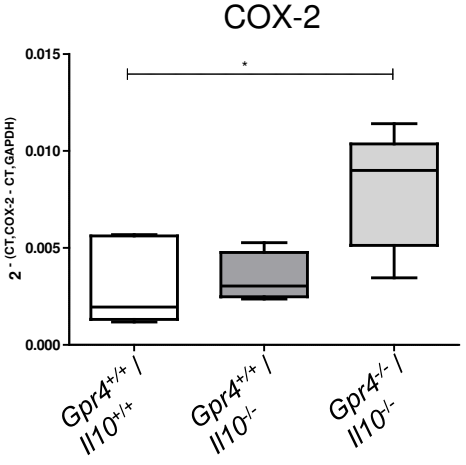

Supplementary Figure 10

Gpr4 in wild type colon

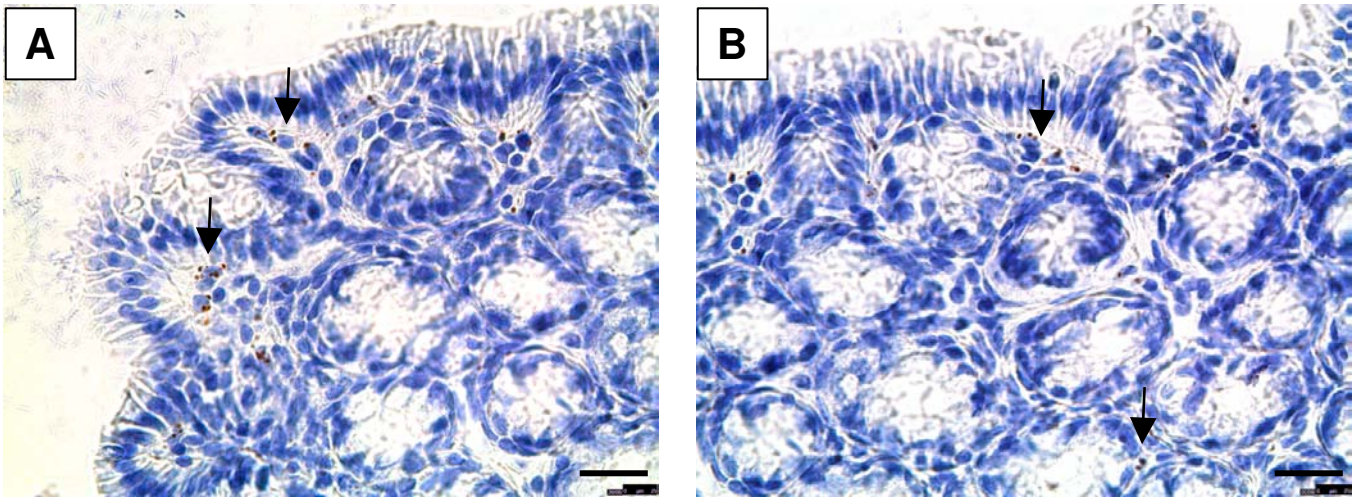

Gpr4 in *Il10*$^{-/-}$ colon

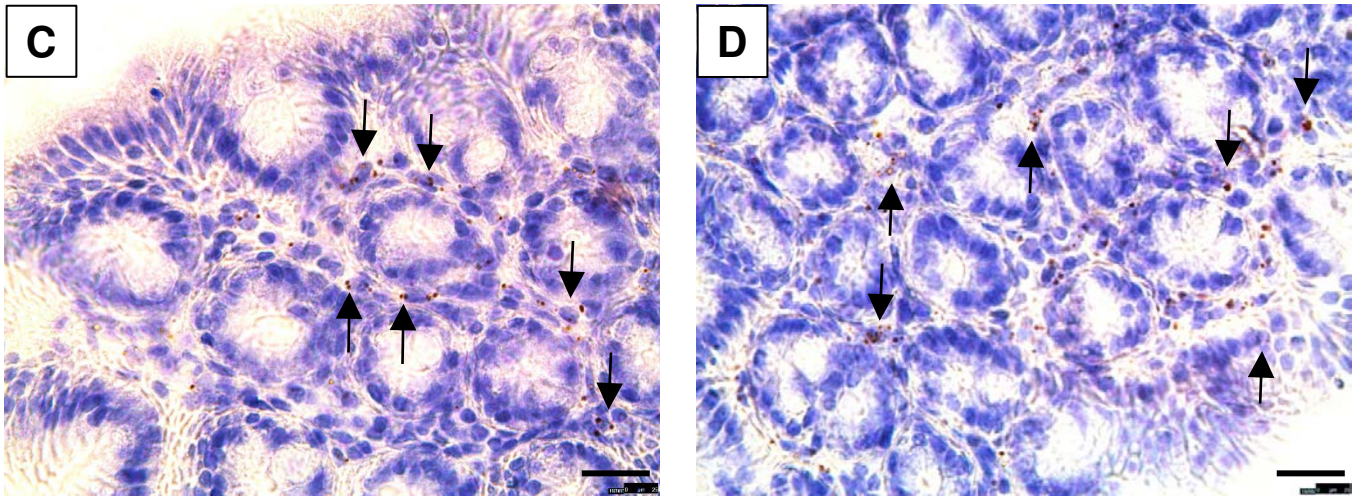

Supplementary Figure 11

Gpr4 mRNA in *Gpr4*$^{-/-}$ colon

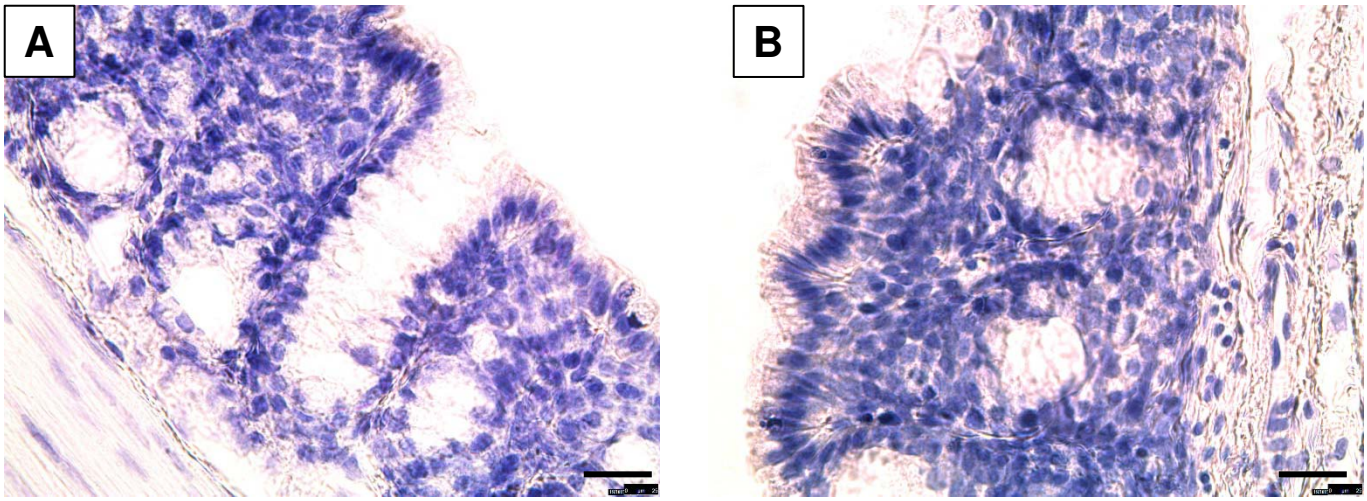

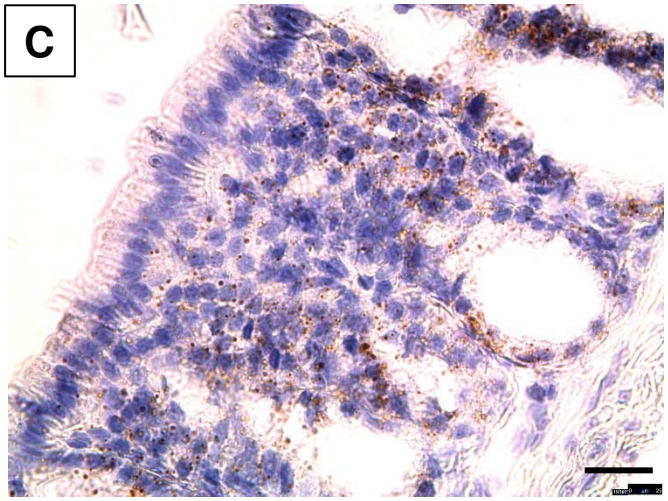

Positive RNAscope control (Peptidyl-prolyl cis-trans isomerase B) in *Gpr4*$^{-/-}$ colon